

Discovery of *S*-[5-Amino-1-(4-fluorophenyl)-1*H*-pyrazol-4-yl]-[3-(2,3-dihydroxypropoxy)phenyl]-methanone (RO3201195), an Orally Bioavailable and Highly Selective Inhibitor of p38 Map Kinase

David M. Goldstein,^{*,†} Tom Alfredson,[†] Jay Bertrand,[‡] Michelle F. Browner,[†] Ken Clifford,[†] Stacie A. Dalrymple,[#] James Dunn,[†] Jose Freire-Moar,^{||} Seth Harris,[†] Sharada S. Labadie,[†] JoAnn La Fargue,[†] Jean Marc Lapierre,[⊥] Susan Larrabee,[†] Fujun Li,[†] Eva Papp,[†] Daniel McWeeney,[†] Chakk Ramesha,[†] Rick Roberts,[†] David Rotstein,[†] Bong San Pablo,[#] Eric B. Sjogren,[†] On-Yee So,[†] Francisco X. Talamas,[†] Will Tao,[†] Alejandra Trejo,[†] Armando Villaseñor,[†] Mary Welch,[†] Teresa Welch,[†] Paul Weller,[†] Phyllis E. Whiteley,[§] Kelly Young,[†] and Sheila Zipfel[#]

Roche Palo Alto LLC, 3431 Hillview Avenue, R6-123, Palo Alto, California 94304, Pharmacia Italy, Pfizer Group, Milan 20014, Italy, Celera Genomics, 180 Kimball Way, South San Francisco, California 94080, Forest Research Institute, Harborside Financial Center, Jersey City, New Jersey 07311, Arqule, Inc., 19 Presidential Way Woburn, Massachusetts 01801, and Perlegen Sciences, Inc., 2021 Stierlin Court, Mountain View, California 94043

Received July 28, 2005

A novel class of highly selective inhibitors of p38 MAP kinase was discovered from high throughput screening. The synthesis and optimization of a series of 5-amino-*N*-phenyl-1*H*-pyrazol-4-yl-3-phenylmethanones is described. An X-ray crystal structure of this series bound in the ATP binding pocket of unphosphorylated p38 α established the presence of a unique hydrogen bond between the exocyclic amine of the inhibitor and threonine 106 which likely contributes to the selectivity for p38. The crystallographic information was used to optimize the potency and physicochemical properties of the series. The incorporation of the 2,3-dihydroxypropoxy moiety on the pyrazole scaffold resulted in a compound with excellent drug-like properties including high oral bioavailability. These efforts identified **63** (RO3201195) as an orally bioavailable and highly selective inhibitor of p38 which was selected for advancement into Phase I clinical trials.

Introduction

Continued interest in development of small molecule inhibitors of p38 MAP kinase is based on the central role this enzyme plays in inflammatory cell signaling. It is known that activation of p38 leads to increased production of pro-inflammatory cytokines such as TNF- α and IL-1 β .¹ Human clinical trials with biologic agents which neutralize TNF (etanercept, infliximab and adalimumab) or IL-1 (anakinra) have validated the concept that modulation of these cytokines leads to dramatic improvement in inflammatory diseases such as RA, psoriasis and inflammatory bowel disease.² While these biologic agents have revolutionized the treatment of some inflammatory disorders, their high cost and inconvenient dosing regimens creates the need for safe and effective orally active inhibitors of TNF and/or IL-1. Several excellent reviews describing the potential importance of p38 inhibitors as novel therapeutics in inflammatory disorders have been published.³ To date, however, only a small number of inhibitors of p38 have been reported to have advanced into phase II clinical trials. Only Vertex has reported a correlation between inhibition of p38 and therapeutic benefit in RA patients.⁴ A number of other agents have established a correlation between inhibition of p38 and inhibition of TNF and/or IL1 in phase I studies in healthy volunteers.⁵

Herein, we describe one part of our overall strategy to identify multiple novel scaffolds as inhibitors of p38 MAP kinase. We

previously reported on the design and synthesis of 4-azaindoles as potent and selective inhibitors of p38.⁶ In this manuscript, we describe our efforts to optimize a lead identified through high throughput screening (HTS), 4-benzoyl-5-aminopyrazole. Several benzoyl containing amino pyrazoles were identified in our HTS campaign, including compound **1** with an IC₅₀ = 2.3 μ M. Early crystallographic efforts resulted in cocrystal structures of the pyrazole series bound to unphosphorylated p38 MAP kinase. These X-ray structures revealed a novel interaction in the ATP binding site. In particular, the amine forms a hydrogen bond with the side chain hydroxyl of threonine 106, a residue not prevalent in most human kinases, which we hypothesized might impart a high degree of selectivity to the series. The structure also identified portions of the lead molecule which could be readily substituted to optimize the physicochemical properties of the series without loss of intrinsic potency. This paper highlights our strategy utilizing structural data to drive lead optimization and to ultimately identify **63** (RO3201195), a highly selective and orally bioavailable inhibitor of p38.

Chemistry

Two synthetic routes to the (5-amino-1-phenyl-1*H*-pyrazol-4-yl)phenylmethanone scaffold were developed (Schemes 1 and 2). The principle approach began with the corresponding methyl benzoate **6**. Addition of the lithium anion derived from acetonitrile provided cyano ketone **7** in good yield. Ketone **7** reacted with *N*-phenylformamidine to form enamine **8** in high yields. Treatment of **8** with the corresponding hydrazine proceeded with high regioselectivity and exclusively cyclized onto the nitrile to form pyrazole compounds **1** and **9–21**.

Alternatively, the pyrazoles could be assembled according to the route highlighted in Scheme 2. This approach allowed the benzoyl ring to be added at a later stage of the synthesis.

* To whom correspondence should be addressed. Phone (650) 855-5413. Fax: (650) 852-1311. E-mail: David-M.Goldstein@roche.com.

[†] Roche Palo Alto LLC.

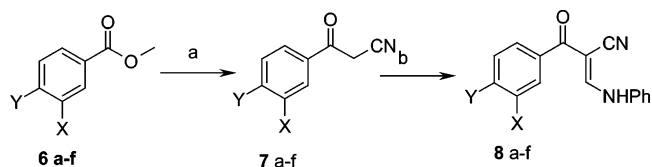
[‡] Pharmacia Italy.

[#] Celera Genomics.

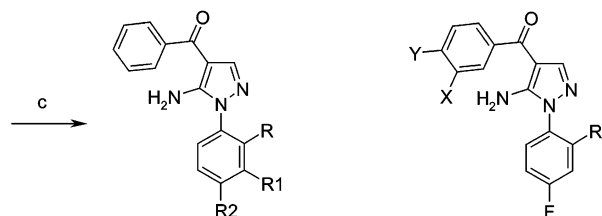
^{||} Forest Research Institute.

[⊥] Arqule, Inc.

[§] Perlegen Sciences, Inc.

Scheme 1. Synthesis of (5-Amino-1-phenyl-1*H*-pyrazol-4-yl)-phenylmethanones (Method A)^a

	X	Y
a	H	H
b	Br	H
c	I	H
d	H	I
e	OCH ₃	H
f	2-morpholin-4-yl-ethoxy	H



	R	R1	R2
1	H	H	H
9	CH ₃	H	H
10	H	NO ₂	H
11	H	H	F
12	H	F	H
13	F	H	H
14	H	H	OCH ₃
15	OCH ₃	H	H

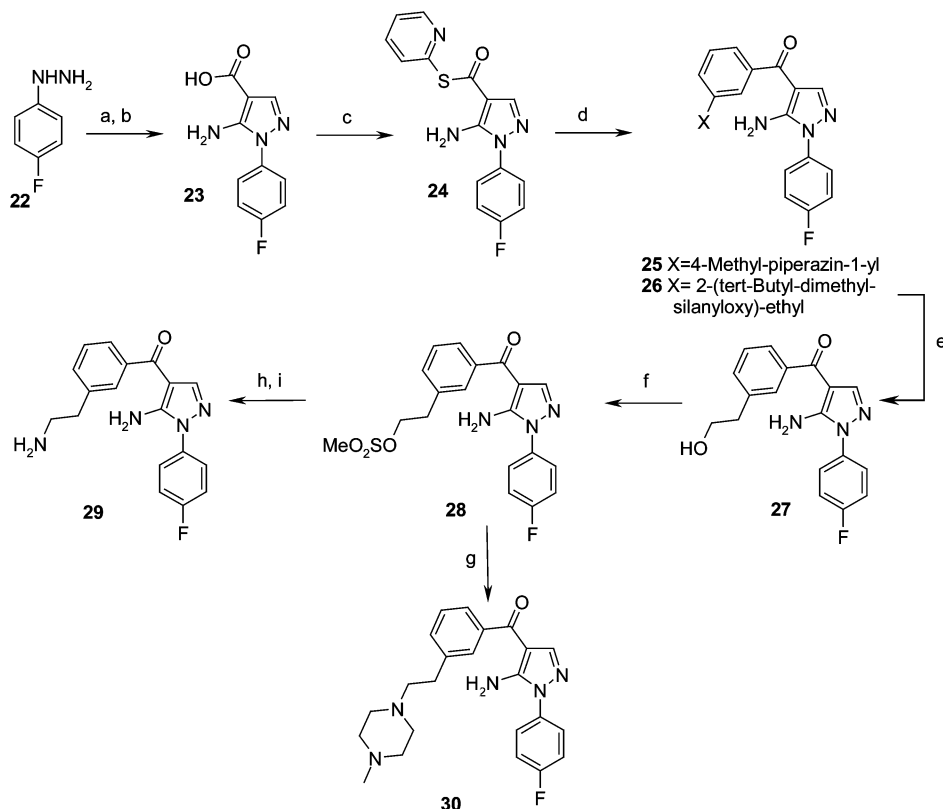
	X	Y	R
16	Br	H	H
17	Br	H	F
18	I	H	H
19	H	I	H
20	OCH ₃	H	H
21	2-morpholin-4-yl-ethoxy	H	H

^a Reagents: (a) CH₃CN, LDA, THF; (b) C₆H₅N:CHNHC₆H₅, xylenes, reflux; (c) appropriately substituted phenylhydrazine, ethanol.

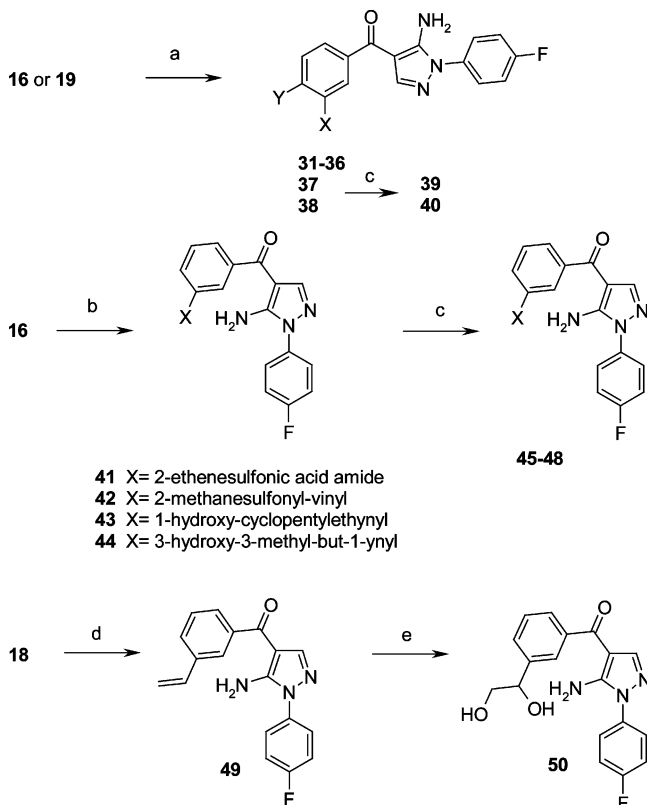
Condensation of ethyl (ethoxymethylene)cyanoacetate with 4-fluorophenyl hydrazine **22** in ethanol formed pyrazole carboxylate esters directly. Saponification of the ester with lithium hydroxide in methanol provided 5-amino-4-carboxypyrazole **23**. Activation of the acid by conversion to the 2-thiopyridyl ester afforded intermediate **24** which was directly reacted with substituted phenylmagnesium bromides in THF⁷ to give ketones **25** and **26**. Subsequent deprotection of the silyl ether with TBAF gave **27** which was then converted to the mesylate **28** under standard conditions. Treatment of **28** with sodium azide and potassium carbonate in DMF,⁸ followed by Staudinger reduction with triphenylphosphine, provided analogue **29**.⁹ Alternatively, nucleophilic displacement of the mesylate **28** with 1-methylpiperazine under basic conditions in DMF gave compound **30**.

Elaboration of the aryl ring using various coupling technologies is described in Schemes 3 and 4. Coupling of aryl halide **16** or **19** with alkynes under Sonogashira coupling conditions¹⁰ gave derivatives **31–38**. Alternatively, Heck reactions with halide **16** provided olefins **41–44** in good yield. Hydrogenations of the unsaturated side chains using catalytic palladium on carbon afforded derivatives **45–48**. Finally, Stille coupling¹¹ with iodide **18** and vinyltributyltin gave styrene **49**. Dihydroxylation of **49** with osmium tetroxide¹² gave the desired diol **50** in good yields.

Alternatively, Suzuki coupling of aryl halides could be used to access compounds **51–58** as described in Scheme 4. Coupling of pyridylboronic acids with halides **16**, **17** or **19** produced compounds **51–55**. The *N*-oxide analogue **56** was produced via oxidation of **55** with *m*CPBA in dichloromethane. Preparation of analogues **57** and **58** started from iodo derivative **18**. Suzuki coupling between (2-bromoallyloxymethyl)benzene and iodide **18** via in situ boronate formation¹³ provided intermediate **57** in

Scheme 2. Synthesis of [5-Amino-1-(4-fluorophenyl)-1*H*-pyrazol-4-yl]-[3-(substituted)phenyl]methanones (Method B)^a

^a Reagents: (a) ethyl (ethoxymethylene)cyanoacetate, ethanol, reflux; (b) LiOH, methanol, reflux; (c) 2,2'-dipyridinyl disulfide, Ph₃P, acetonitrile; (d) RPhMgBr or RPhLi, THF; (e) TBAF, THF, room temp; (f) CH₃SO₂Cl, pyridine, room temp; (g) 1-methylpiperazine, K₂CO₃, DMF, 70 °C; (h) NaN₃, K₂CO₃, DMF, room temp; (i) Ph₃P, THF.

Scheme 3. Synthesis of [5-Amino-1-(4-fluorophenyl)-1*H*-pyrazol-4-yl]-[3-(substituted)phenyl]methanones^a

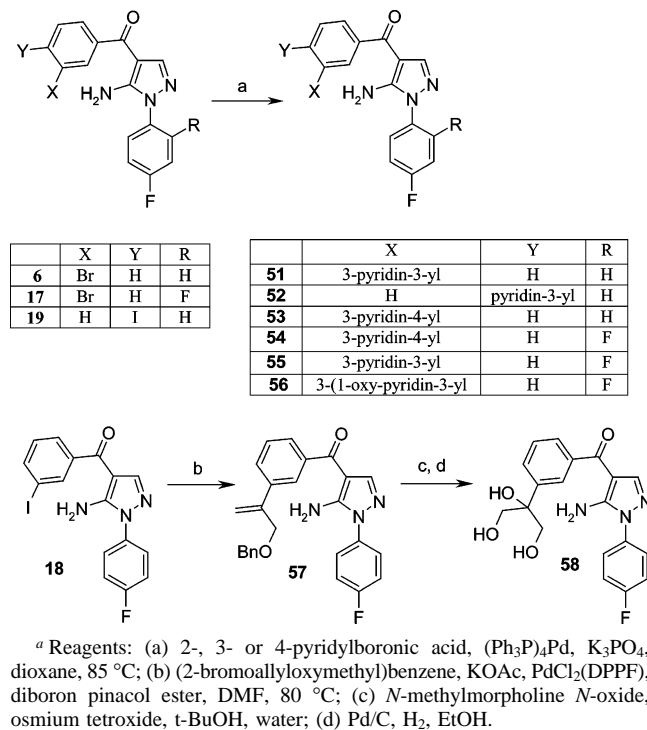
^a Reagents: (a) Zn(CN)₂, (Ph₃P)₄Pd, DMF, 60 °C or alkyne, (Ph₃P)₂PdCl₂, CuI, diisopropylamine, 70 °C; (b) triethylamine, (Ph₃P)₂PdCl₂, DMF, 100 °C; (c) Pd/C, H₂, EtOAc, EtOH, room temp; (d) vinyltributyltin, (Ph₃P)₄Pd, DMF, 100 °C; (e) *N*-methylmorpholine *N*-oxide, osmium tetroxide, *t*-BuOH.

acceptable yield. Subsequent oxidation with osmium tetroxide followed by catalytic hydrogenation to remove the benzyl protecting group furnished compound **58**.

Preparation of oxygen linked derivatives is shown in Scheme 5. Deprotection of the methoxy group of **20** with boron tribromide provided phenol **59** which served as an intermediate for the preparation of analogues **61–63**. Analogue **61** was prepared by Mitsunobu coupling of phenol **58** with bromoethanol followed by subsequent halide displacement with piperidine. Alternatively, alkylation of phenol **59** with (*R*)- or (*S*)-*O*-isopropylidene-glycerol tosylate followed by deprotection of the acetal with *p*-toluenesulfonic acid gave chiral alcohols **62** and **63**.

Results and Discussion

Initial Lead Identification. HTS was performed using a radioactive filtration binding format using [³³P] ATP (250 μM) and myelin basic protein (150 μM) as the substrate. Compounds were initially tested at 40 μM, and those which displayed >40% inhibition of the enzyme activity were retested in the same format at multiple concentrations. Several benzoyl amino pyrazoles were identified in our HTS campaign, including compound **1**, which was confirmed to have an IC₅₀ = 2.3 μM. To our knowledge, this was the first example of this scaffold to be identified as an inhibitor of a protein kinase. Preliminary SAR studies revealed that only small hydrophobic substituents on the *N*-phenylpyrazole ring were tolerated (Table 1). It was found that substitution at the para position of the phenyl ring (compare ortho (**13**) vs meta (**12**) vs para (**11**) fluorine derivatives and ortho (**15**)/para (**14**) methoxy) was preferred.

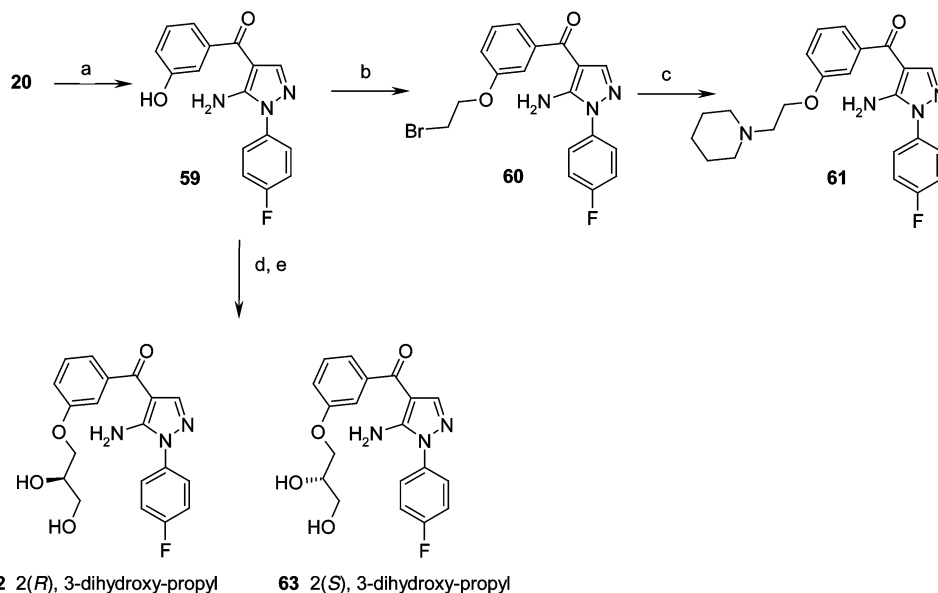
Scheme 4. Synthesis of [5-Amino-1-(4-fluorophenyl)-1*H*-pyrazol-4-yl]-[3-(substituted)phenyl]methanones^a

^a Reagents: (a) 2-, 3- or 4-pyridylboronic acid, (Ph₃P)₄Pd, K₃PO₄, dioxane, 85 °C; (b) (2-bromoallyloxymethyl)benzene, KOAc, PdCl₂(DPPF), diboron pinacol ester, DMF, 80 °C; (c) *N*-methylmorpholine *N*-oxide, osmium tetroxide, *t*-BuOH, water; (d) Pd/C, H₂, EtOH.

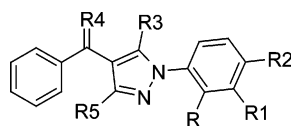
More polar residues such as nitro and methoxy were less active than hydrogen. In parallel, attempts to replace the exocyclic amine resulted in loss of activity. Likewise, conversion of the ketone to an oxime also resulted in inactive compounds.

X-ray Crystallography. To accelerate optimization of the pyrazole lead series, significant effort was focused on generation of X-ray crystal structures of pyrazole analogues bound to p38α enzyme. The X-ray crystal structures of p38 MAP kinase with bound pyrazole compounds revealed a unique binding motif previously not reported for inhibitors of p38 kinase (Figure 1). This class of inhibitors form a hydrogen bond between the benzoyl oxygen and the main chain NH of methionine 109 (1.8 Å), a key interaction observed with all ATP competitive p38 inhibitors (Figure 1b). A novel hydrogen bond was observed between the NH₂ group of the aminopyrazole and the side chain alcohol of threonine 106. A hydrogen bond between a p38 inhibitor and threonine 106 has not been reported previously. With only approximately 20% of the human kinome having a threonine at this position, we hypothesized that an inhibitor series with this unique interaction could confer improved selectivity versus other kinases which do not contain a similarly located threonine. The *N*-phenyl ring of this inhibitor class is positioned in a hydrophobic pocket toward the back of the binding site, which is partially defined by threonine 106.

Lead Optimization Strategy. Compounds derived from the pyrazole series were extremely insoluble and had poor oral bioavailability. It was clear from the initial X-ray structures that substitution of the benzoyl ring at either the meta or para position would be well tolerated by the protein (Figure 1a). We anticipated that substitutions at this position would be required to achieve the desired physical properties for the series. Our basic strategy was to improve the potency of the lead compounds based on data from in vitro assays and then to optimize the pharmacokinetic properties. We put particular emphasis on the LPS-induced cytokine production assay in undiluted human whole blood (HWB) as a key driver for compound selection as this assay provided surrogate efficacy in a physiologically

Scheme 5. Synthesis of [5-Amino-1-(4-fluorophenyl)-1*H*-pyrazol-4-yl]-(3-hydroxy-substituted-phenyl)methanones^a

^a Reagents: (a) BBr_3 , CH_2Cl_2 , room temp; (b) 2-bromoethanol, Ph_3P , diethyl azodicarboxylate, toluene, 0 °C room temp; (c) piperidine, ethanol, reflux; (d) (*R*)-*O*-isopropylidene glycerol tosylate or (*S*)-*O*-isopropylidene glycerol tosylate, K_2CO_3 , DMF, 80 °C; (e) *p*-toluenesulfonic acid monohydrate, water, 50 °C.

Table 1. In Vitro Activity of 2–15 versus Compound 1

	R	R1	R2	R3	R4	R5	$\text{P}_{38\alpha}$, $\text{IC}_{50}^a \pm \text{ASE} (\mu\text{M})$	THP-1 TNF- α , $\text{IC}_{50} \pm \text{ASE} (\mu\text{M})$
1	H	H	H	NH_2	O	H	2.30 ± 0.6	0.57 ± 0.05
2	H	H	H	CN	O	H	> 100	
3	H	H	H	OH	O	CH_3	> 100	
4	H	H	H	NH_2	N- OCH_3	H	51 ± 12	> 18
5	H	H	H	NH_2	N- OCH_3	H	> 100	> 18
9	CH_3	H	H	NH_2	O	H	1.08 ± 0.16	0.51 ± 0.09
10	H	NO_2	H	NH_2	O	H	64.2 ± 30.6	> 56
11	H	H	F	NH_2	O	H	1.10 ± 0.11	0.10 ± 0.04
12	H	F	H	NH_2	O	H	6.7 ± 0.96	1.59 ± 0.47
13	F	H	H	NH_2	O	H	2.86 ± 0.21	0.56 ± 0.02
14	H	H	OCH_3	NH_2	O	H	7.06 ± 0.44	0.64 ± 0.06
15	OCH_3	H	H	NH_2	O	H	8.38 ± 2.5	0.53 ± 0.12

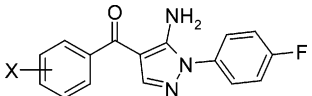
^a IC_{50} s were calculated from the dose–response curves. Positive control: 4-[5-(4-Fluorophenyl)-4-pyridin-4-yl-1*H*-imidazol-2-yl]phenol, compound 64 (SB202190),²⁰ IC_{50} of $0.03 \pm 0.003 (\mu\text{M})$.

relevant environment in the presence of serum albumin and other proteins. Initial focus was to install either polar or ionizable functional groups to either the para or the meta position of the aryl ring either directly or via a linker group of different lengths. It became apparent after synthesis of a number of analogues that the meta position offered significantly greater tolerability to a wide range of substituents than the corresponding para-substituted analogues (examples include meta-substituted compounds 31, 37 and 39 vs para analogues 32, 38 and 40). While it was not immediately evident from our X-ray structures why there was a preference for meta substitution, we focused our optimization on a broader range of substituents at the meta position. The installation of ionizable function, as expected, did lead to dramatic improvements in intrinsic solubility; an increase in solubility from 1 to 5 $\mu\text{g}/\text{mL}$ in the lead molecule to >6 mg/mL and 5–10 mg/mL was obtained with analogues 25 and 36 respectively. This prompted us to explore other basic containing groups (Table 2). While these derivatives had desirable solubilities, they also exhibited greater inhibition in cellular assays than expected based on their intrinsic in vitro

enzyme potency. We postulated that these molecules may have other nonspecific effects resulting in cytotoxicity. In addition, compounds such as 21 suffered from problems such as poor metabolic stability and/or a complex metabolic profile specific to the amine-bearing side chains. We ultimately chose to look for alternate ways to improve the physicochemical properties including installation of less-basic amines which would be uncharged at physiologic pH. To this end, another series of pyridyl analogues were synthesized and the results are shown in Table 3. Within this series, several analogues were identified that had enhanced potency with a similar correlation between the isolated enzyme and the cellular assays as observed with the more basic amine derivatives. While these compounds showed good metabolic stability (only the *N*-oxide metabolite of the pyridyl ring was identified, data not shown), they unfortunately exhibited toxicity upon chronic administration in rodents.

On the basis of these findings, alternate nonionizable solubilizing functional groups became the primary focus of the lead optimization strategy (Table 4). A variety of polar functional

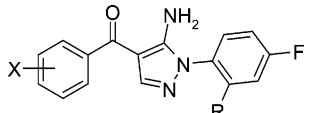
Table 2. Basic Amines as Solubilizing Groups



	X	P _{38α} , IC ₅₀ ^a ± ASE (μM)	THP-1 TNF-α, IC ₅₀ ± ASE (μM)	aqueous solubility (mg/mL)
21	3-(2-morpholin-4-ylethoxy)	1.27 ± 0.5	0.37 ± 0.02	>200
25	4-methylpiperazin-1-yl	2.00 ± 0.3	1.21 ± 0.19	>6
29	2-aminoethyl	2.44 ± 0.8	0.52 ± 0.05	>10
30	2-(4-methylpiperazin-1-yl)ethyl	1.64 ± 0.3	0.36 ± 0.12	1
31	3-cyano	4.76 ± 1.4	2.78 ± 0.9	
32	4-cyano	8.38 ± 3.5	>30	
33	3-(3-hydroxyprop-1-ynyl)	4.04 ± 0.67	0.21 ± 0.03	
34	3-dimethylaminoprop-1-ynyl	2.28 ± 0.7	0.15 ± 0.01	
35	3-(4-methylpiperazin-1-yl)	2.65 ± 0.3	0.78 ± 0.18	
36	3-piperidin-1-ylprop-1-ynyl	1.32 ± 0.18	0.06 ± 0.01	5–10
37	3-(3-morpholin-4-ylprop-1-ynyl)	1.72 ± 0.3	0.13 ± 0.01	
38	4-(3-morpholin-4-ylprop-1-ynyl)	3.13 ± 0.8	11.22 ± 2.4	
39	3-(3-morpholin-4-ylpropyl)	1.74 ± 0.4	1.04 ± 0.09	
40	4-(3-morpholin-4-ylpropyl)	22.3 ± 4.4		
61	2-piperidin-1-ylethoxy	1.84 ± 0.6	1.41 ± 0.19	

^a IC₅₀s were calculated from the dose–response curves. Positive control: Compound **64**. IC₅₀ of 0.03 ± 0.003 (μM).

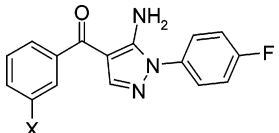
Table 3. Pyridyl Substitution



	X	R	P _{38α} , IC ₅₀ ^a ± ASE (μM)	THP-1 TNF-α, IC ₅₀ ± ASE (μM)	aqueous solubility, μg/mL
51	3-pyridin-3-yl	H	0.78 ± 0.25	0.047 ± 0.005	18.1
52	4-pyridin-3-yl	H	0.98 ± 0.2	0.17 ± 0.03	
53	3-pyridin-4-yl	H	1.28 ± 0.3	>10	
54	3-pyridin-4-yl	F	0.31 ± 0.04	0.03 ± 0.003	1.4
55	3-pyridin-3-yl	F	0.18 ± 0.03	0.04 ± 0.005	10.7
56	3-(1-oxypyridin-3-yl)	F	0.34 ± 0.04	0.04 ± 0.01	5.8

^a IC₅₀s were calculated from the dose–response curves. Positive control: Compound **64**. IC₅₀ of 0.03 ± 0.003 (μM).

Table 4. Nonbasic Functional Groups as Solubilizing Agents



	X	P _{38α} , IC ₅₀ ^a ± ASE (μM)	THP-1 TNF-α, IC ₅₀ ± ASE (μM)	HWB IL-1, IC ₅₀ ± ASE (μM)	aqueous solubility, μg/mL
27	2-hydroxyethyl	0.85 ± 0.5	0.19 ± 0.03	0.69 ± 0.13	
45	2-ethanesulfonic acid amide	1.25 ± 0.1	0.51 ± 0.02	3.60 ± 0.6	5.6
46	2-methanesulfonylethyl	0.79 ± 0.25	0.52 ± 0.03	0.22 ± 0.03	121
47	2-(1-hydroxycyclopentyl)ethyl	0.23 ± 0.07	0.13 ± 0.007	4.64 ± 0.4	0.7
48	3-hydroxy-3-methylbutyl	0.59 ± 0.18	6.59 ± 0.18	0.92 ± 0.13	ca. 40
50	1,2-dihydroxyethyl	3.5 ± 0.8	1.30 ± 0.12	1.20 ± 0.36	>300
58	1,2-dihydroxy-1-hydroxymethylethyl	9.54 ± 4.4	>10		
62	2,3-dihydroxypropoxy	1.20 ± 0.4	0.2 ± 0.04	0.76 ± 0.4	36.2
63	2,3-dihydroxypropoxy	0.7 ± 0.1	0.25 ± 0.01	0.57 ± 0.04	35.4

^a IC₅₀s were calculated from the dose–response curves. Positive control: Compound **64**. IC₅₀ of 0.03 ± 0.003 (μM).

derivatives were made including amides, sulfonamides, ethers, alcohols and diols. While several functionalities maintained excellent potency against p38, only a few derivatives retained both intrinsic potency as well as good inhibition of LPS-induced IL-1β production in undiluted human whole blood. The compounds which had the best balance between desirable physical properties and potency in both in vitro and acute in vivo assays were compounds **27** and **46** and diols **62** and **63**. As there was no precedence for the use of diols as solubilizing groups for kinase inhibitors, there was some concern that these diols would be prone to rapid clearance in vivo. We chose to evaluate **27**

and **46** and both enantiomers **62** and **63** in vivo to evaluate their pharmacokinetic properties. Definitive PK studies ultimately resulted in the selection of diol **63** (the *S* enantiomer) due to its high bioavailability and lower clearance rates relative to the (*R*) enantiomer and analogues **27** and **46** across multiple species

Pharmacokinetics and Metabolism of 63. A summary of the pharmacokinetic parameters for the *S* isomer **63** is detailed in Table 5. In animals, systemic clearance of **63** was low to moderate, while volume of distribution (*V*_{dss}) was medium to high. The absorption was rapid and complete. Oral bioavailability was 62%, 57% and 88% in rat, monkey and dog,

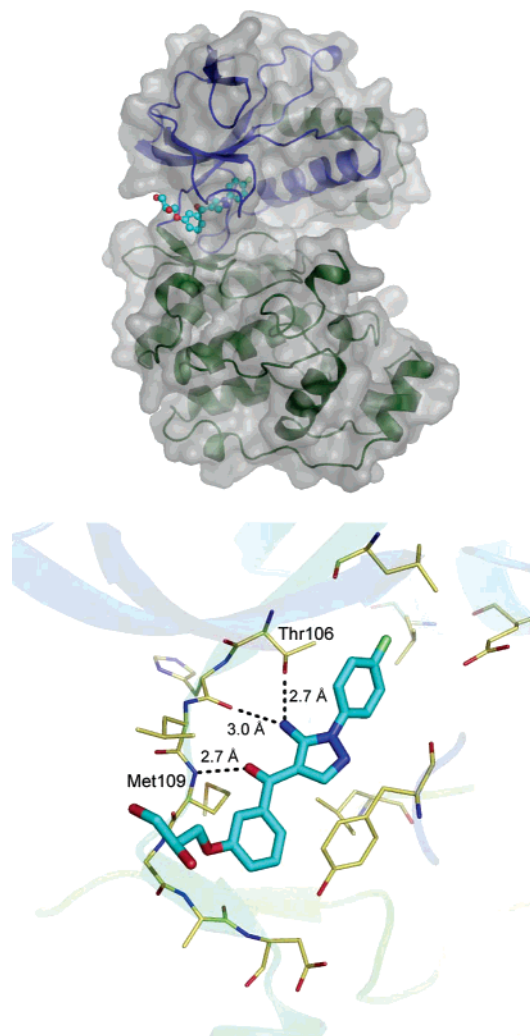


Figure 1. X-ray crystal structure of compound **63** bound in the ATP binding site of unphosphorylated p38 MAP kinase. A. Ribbon diagram of the p38 MAP kinase with the N-terminal domain colored blue and the C-terminal domain in green. Substitutions at the meta or para positions of the benzoyl ring are well tolerated because of their location outside of the surface enclosed binding site. The enzyme is represented by a transparent representation of the enzyme surface. B. Close-up of the inhibitor binding to p38 MAP kinase. Hydrogen bond interactions between the pyrazole and protein atoms are indicated, including the novel interaction with side chain of threonine 106. This interaction may be critical for the observed kinase selectivity of this class of inhibitors.

respectively. Compound **63** was moderately bound (79–88%) to plasma in all species studied. In vitro, **63** is a poor substrate for cytochrome P-450 and had a low affinity for the major isoforms. In inhibition studies with human cytochrome P-450 enzymes, **63** modestly inhibited only the 2C9 isoform with an IC_{50} of 11 μ M (IC_{50} values for human cytochromes 1A2, 2C19, 2D6 and 3A4 were greater than 25 μ M).

Pharmacological Evaluation of 63. The complete in vitro and in vivo pharmacology for diol **63** is summarized in Table 6. Compound **63** decreased the production of secreted cytokines such as TNF α in a human monocytic cell line, THP1, after stimulation with LPS. Compound **63** showed a concentration-dependent inhibition of TNF α production with an estimated IC_{50} of 0.25 μ M. The inhibitory effect of **63** on TNF α and IL-1 β production also was tested in a mononuclear cell fraction isolated from HWB. Inhibitor **63** displayed a similar concentration-dependent inhibition for both IL-1 β and TNF α . The concentration-dependent inhibition of IL-1 β was comparable to the

Table 5. Single Dose Plasma Pharmacokinetic Parameters of **63** Following Dosing in Animals

	species, strain		
	rat, Hanover–Wistar	monkey, cyno-molgus	dog, beagle
dose (mg/kg)	10	10	10
gender	males	male	female
sample size (iv, po)	60, ^a 15 ^b	4, 3 ^b	4, 3 ^b
po T_{max} (h)	3	1.08	0.83
po C_{max} (μ g/mL)	4.48	2.02	4.21
po $T_{1/2}$ (h)	1.64	2.41	1.57
po AUC Inf (μ g·h/mL)	19.50	7.56	13.30
po $F\%$	61.70	56.80	87.50
iv Cl (L/h/kg)	0.32	0.76	0.67
iv V_{dss} (L/kg)	1.27	21.40	2.55
% protein binding ^c	12.10	11.20	21.30

^a iv values based on mean plasma concentrations; plasma from three rats per sample time. ^b Values based on mean parameter; serial plasma samples obtained from each animal. ^c The in vitro binding of [¹⁴C]-**63** to plasma protein at 37 °C was studied by ultrafiltration methods.

inhibition detected in the unfractionated whole blood, whereas TNF α was more potently inhibited in the mononuclear cell fraction. To evaluate **63** in vivo, the compound was tested in a number of acute inflammatory models. In the first study, **63** was dosed orally and was evaluated for its ability to inhibit the production of TNF α and IL-6 after IP injection of LPS into Hanover–Wistar and Sprague–Dawley rats. In this model, **63** was administered to rats 0.5 h prior to challenge with 50 μ g/kg LPS. Serum was collected 1.5 h after LPS injection for analysis of cytokines and concentrations of drug. Compound **63** demonstrated significant dose-dependent inhibition of serum TNF α and IL-6. The estimated effective dose (ED) for TNF α inhibition by **63** is reported in Table 6. In addition to inhibition of TNF α production, compound **63** also regulates TNF α signaling. In another rat model, **63** was administered to rats 0.5 h prior to challenge with TNF α . Serum was collected 2 h after IP injection of TNF α for analysis of cytokines and concentrations of drug. Compound **63** inhibited TNF α -induced IL-6 at an $ED_{50} \pm ASE$ of 1.5 ± 0.5 mg/kg. Furthermore, compound **63** was evaluated in a chronic disease model, rat adjuvant arthritis (AI), by subcutaneous delivery using osmotic minipumps. Lewis rats were treated with vehicle or compound **63** delivered at a rate of 0.5 mg/hr from day 1 to 14. Compound **63** inhibited the adjuvant-induced increase in hind paw weight by 58% ($p < 0.01$) compared to vehicle-treated animals. In addition, the mean clinical score exhibited by compound **63** treated rats was 6 (± 1) compared to 10 (± 0.7) out of a possible 19 in vehicle-treated rats ($p < 0.05$). Plasma concentrations of compound **63** were 7.6 ± 0.8 and 7.5 ± 0.6 μ M (mean \pm SEM) on days 3 and 14, respectively.

Kinase Selectivity Profiling. Protein kinases are considered “higher” risk drug discovery targets in part due to the difficulty to both measure and achieve kinase selectivity. We have continued to improve our ability to assess the kinase selectivity and to correlate the profiles of our kinase inhibitors with their in vitro and in vivo pharmacology. As part of these efforts, we evaluated the in vitro kinase selectivity profile of **63** against 105 kinases using the Ambit Biosciences platform.¹⁴ Of the 105 kinases tested, **63** inhibited only six other kinases with inhibition $> 50\%$ at 10 μ M concentration. For each of these kinases, the K_d was determined as is reported in Table 7. Compound **63** is highly selective for p38 and inhibits only two other kinases at comparable concentrations to its p38 activity. Compound **63** binds to both p38 α and p38 β isoforms but does not bind to either the p38 γ or p38 δ isoforms. Compound **63** binds to both

Table 6. Summary of Biological Efficacy of Analogue **63**

	in vitro					in vivo			
	THP-1 ^a	HWB ^a		mononuclear ^b		LPS ^c	LPS ^c	TNF α ^c	AI
	TNF α	TNF α	IL-1 β	TNF α	IL-1 β	TNF α	IL-6	IL-6	paw weight
IC ₅₀ (μ M) or [plasma] (μ M)	0.25 \pm 0.01	1.97 \pm 0.1	0.57 \pm 0.04	0.4 \pm 0.1	0.5 \pm 0.1				[7.5 \pm 0.6]
ED ₅₀ (mg/kg)						0.2 \pm 0.04	0.3 \pm 0.05	1.5 \pm 0.5	
% inhibition (vs vehicle)									58, <i>p</i> < 0.01

^a The data are expressed as the combined mean IC \pm SEM. ^b The data are expressed as the mean IC \pm ASE. ^c The data are expressed as the mean ED \pm SEM.

Table 7. Kinases Inhibited by Compound **63** from a Panel of 105 Kinases Tested at 10 μ M

kinase	kinase assay K _d ^a (μ M)
EPHA5	6.6
GAK	0.59
JNK2	5.0
JNK3	6.9
LCK	3.8
PDGFR β	0.61
P38 α	0.20
P38 β	0.05

^a The K_ds were determined using the Ambit Bioscience platform.¹⁴

the phosphorylated and unphosphorylated form of p38 α (data not shown) as commonly reported for ATP competitor inhibitors of p38.

On the basis of all of these results, compound **63** was selected as a candidate for Phase I clinical trials as an oral agent that will suppress TNF and related cytokine production, with the potential to offer increased safety and efficacy compared to the current standard therapies for RA at appreciably less cost than that of biological anticytokine therapy.

Conclusion

A novel class of p38 inhibitors (5-amino-1-phenyl-1*H*-pyrazol-4-yl)phenylmethanones was identified by HTS. Initial SAR studies and the cocrystal structure of **25** with unphosphorylated p38 guided our efforts to improve both in vitro and in vivo potency as well as the physical properties of our initial lead. After surveying a wide variety of different solubilizing groups, only nonbasic solubilizing groups, particularly 2(*S*) glycerol monoether **63**, resulted in a balance of good potency and favorable drug delivery characteristics with a desirable metabolic profile. To our knowledge, compound **63** represents the first use of a diol moiety as a solubilizing group for a kinase inhibitor selected for clinical study. Our data suggests that diols can be effectively used to improve the physical properties of otherwise insoluble kinase scaffolds. The use of the glycerol mono ether moiety on the pyrazole scaffold resulted in a molecule with excellent drug-like properties and high oral bioavailability while maintaining intrinsic potency against p38. Compound **63** selectively inhibits p38 MAP kinase, an enzyme in the intracellular signaling pathway for the generation of TNF α and IL-1 β . The compound reduced the production of TNF α from human monocytes, whole blood, and a monocytic cell line in vitro as well as reduced the production of downstream cytokine IL-6 in vivo. Upon the basis of the range of efficacy in the biological models, compound **63** was selected as a clinical candidate for the treatment of inflammatory diseases including rheumatoid arthritis.

Experimental Section

Reagents and solvents were obtained from commercial suppliers and were used without further purification. Flash chromatography was performed with Merck silica gel 60 (230–400 mesh), and

reaction progress was determined by thin-layer chromatography (TLC) using Analtec 250- μ m silica gel plates. Visualization was done with UV light (254 nm) or iodine. Yields are of purified compounds and were not optimized. ¹H NMR measurements were recorded at 75.40 MHz using a Bruker AMX 300 instrument in DMSO with tetramethylsilane as the internal standard. Melting points recorded were uncorrected. Elemental analyses were within \pm 0.4% except for compound **50** for which hydrogen analysis exhibits \pm 0.41% error. Purity of compounds **9–15** and **19** was determined using a Micromass Platform LC, single quadrupole mass spectrometer with an electrospray (ES) probe using a mobile phase of acetonitrile/water with 0.1% TFA.

(5-Amino-1-phenyl-1*H*-pyrazol-4-yl)phenylmethanone (1). A solution of benzoylacetonitrile (10 g, 68.9 mmol) and *N,N*-diphenylformamidine (13.5 g, 68.9 mmol) in xylenes (50 mL) was heated at reflux under argon. After 2 h, the reaction mixture was cooled to room temperature and diluted with ether to give 2-benzoyl-3-phenylaminoacrylonitrile (14.0 g) as a solid.

A mixture of 2-benzoyl-3-phenylaminoacrylonitrile (14.0 g, 56.4 mmol) and phenylhydrazine (5.6 mL, 56.4 mmol) in ethanol (10 mL) was heated at reflux. After 3 h, the reaction mixture was cooled to room temperature and the solid was filtered and washed with ethanol to give (5-amino-1-phenyl-1*H*-pyrazol-4-yl)phenylmethanone (4.75 g). ¹H NMR (DMSO-*d*₆) δ 7.19 (s, 2H), 7.42–7.60 (m, 8H), 7.77–7.80 (m, 2H), 7.81 (s, 1H). Ms (EI/CI) *m/z*: (M + H) 262. Anal. (C₁₆H₁₃N₃O) C, H, N.

4-Benzoyl-2-phenyl-2*H*-pyrazole-3-carbonitrile (2). To a mixture of anhydrous copper bromide (2.3 g, 10.3 mmol) and *tert*-butyl nitrite (1.54 mL, 12.9 mmol) in anhydrous acetonitrile (5 mL) at 65 °C was added 5-amino-1-phenyl-1*H*-pyrazol-4-yl)phenylmethanone (2.3 g, 8.6 mmol) as a solid. The reaction mixture was stirred for 24 h, cooled to room temperature, poured into 2 N HCl (100 mL) and extracted into ethyl acetate, the organic phase was washed with brine, dried over sodium sulfate and concentrated in vacuo and the residue was purified by flash chromatography, eluting with 10–40% ethyl acetate/hexane to afford (5-bromo-1-phenyl-1*H*-pyrazol-4-yl)phenylmethanone (1.25 g).

A mixture of (5-bromo-1-phenyl-1*H*-pyrazol-4-yl)phenylmethanone (900 mg, 2.75 mmol) and CuCN (370 mg, 4.13 mmol) in NMP (100 mL) was refluxed for 2 h and then cooled to room temperature, and an excess of ethylenediamine and ethyl acetate was added. This resulting mixture was filtered through Celite. The filtrate was washed with water and brine and then dried over sodium sulfate. Concentration in vacuo and purification by flash chromatography with 10–40% ethyl acetate/hexane afforded 4-benzoyl-2-phenyl-2*H*-pyrazole-3-carbonitrile (460 mg). ¹H NMR (DMSO-*d*₆) δ 7.61–7.78 (m, 6H), 7.82–7.85 (m, 2H), 7.95–7.98 (m, 2H), 8.45 (s, 1H). Ms (EI/CI) *m/z*: (M + H) 273. Anal. (C₁₇H₁₁N₃O) C, H, N.

(5-Hydroxy-3-methyl-1-phenyl-1*H*-pyrazol-4-yl)phenylmethanone (3). A suspension of 1-phenyl-3-methyl-5-pyrazolone (95.9 g, 28.7 mmol) in dioxane (30 mL) was heated and stirred with an overhead stirrer. When the mixture was homogeneous, calcium hydroxide (4.0 g, 54.0 mmol) was added portion wise followed by dropwise addition of benzoyl chloride (3.3 mL, 28.4 mmol). The mixture was heated at reflux under nitrogen for 30 min, cooled to room temperature and then poured into 2 N HCl (100 mL). The brown solid formed was filtered and purified by flash chromatography eluting with 10–25% ethyl acetate/hexane. ¹H NMR (DMSO-

d_6) δ 2.50 (s, 3H), 7.29–7.34 (m, 1H), 7.46–7.52 (m, 4H), 7.54–7.60 (m, 1H), 7.69–7.76 (m, 4H). MS (EI/CI) m/z : (M + H) 278. Anal. (C₁₇H₁₄N₂O₂) C, H, N.

(5-Amino-1-phenyl-1H-pyrazol-4-yl)phenylmethanone O-Methyloxime (4 and 5). (5-Amino-1-phenyl-1H-pyrazol-4-yl)phenylmethanone (250 mg, 0.95 mmol) in methanol (5 mL) with methoxylamine hydrochloride (95 mg, 1.14 mmol) was treated with pyridine (0.36 mL). The mixture was refluxed for 5 days and then concentrated in vacuo, and the residue was partitioned between water (10 mL) and ethyl acetate (10 mL), separated and extracted with ethyl acetate (2 × 10 mL). The combined organic layers were washed with brine (10 mL) and then dried over sodium sulfate, concentrated in vacuo and purified by preparative thin-layer chromatography eluting with 3:1 hexane/ethyl acetate to afford **4** (84 mg). ¹H NMR (DMSO- d_6) δ 3.88 (s, 3H), 5.47 (br, 2H), 7.05 (s, 1H), 7.35–7.56 (m, 8H), 7.57–7.64 (m, 2H). MS (EI/CI) m/z : (M + H) 294. Anal. (C₁₇H₁₆N₄O) C, H, N and **5** (140 mg) ¹H NMR (DMSO- d_6) δ 4.09 (s, 3H), 4.55 (br, 2H), 7.36–7.46 (m, 5H), 7.47–7.67 (m, 6H). MS (EI/CI) m/z : (M + H) 294. Anal. (C₁₇H₁₆N₄O) C, H, N.

(5-Amino-1-O-tolyl-1H-pyrazol-4-yl)phenylmethanone (9). ¹H NMR (DMSO- d_6) δ 2.11 (s, 3H), 6.89 (s, 2H), 7.33–7.62 (m, 7H), 7.77–7.80 (m, 3H). MS (EI/CI) m/z : (M + H) 278.

[5-Amino-1-(3-nitrophenyl)-1H-pyrazol-4-yl]phenylmethanone (10). ¹H NMR (DMSO- d_6) δ 7.42 (s, 2H), 7.53–7.61 (m, 3H), 7.77–7.89 (m, 4H), 8.07 (d, J = 8.03 Hz, 1H), 8.28 (d, J = 8.27, 1H), 8.38–8.39 (m, 1H). MS (EI/CI) m/z : (M + H) 309

[5-Amino-1-(4-methoxyphenyl)-1H-pyrazol-4-yl]phenylmethanone (14). ¹H NMR (DMSO- d_6) δ 7.02 (s, 2H), 7.10 (d, J = 8.94 Hz, 2H), 7.47 (d, J = 8.96 Hz, 2H), 7.50–7.58 (m, 3H), 7.76–7.78 (m, 3H). MS (EI/CI) m/z : (M + H) 294.

[5-Amino-1-(2-methoxyphenyl)-1H-pyrazol-4-yl]phenylmethanone (15). ¹H NMR (DMSO- d_6) δ 3.83 (s, 3H), 6.85 (s, 2H), 7.10 (t, J = 7.60 Hz, 1H), 7.26 (d, J = 7.38 Hz, 1H), 7.36 (dd, J = 6.09 Hz, J = 1.70 Hz, 1H), 7.48–7.59 (m, 4H), 7.74 (s, 1H), 7.75–7.79 (m, 2H). MS (EI/CI) m/z : (M + H) 294.

[5-Amino-1-(4-fluorophenyl)-1H-pyrazol-4-yl]-(3-bromophenyl)methanone (16). *n*-Butyllithium (214 mL, 340 mmol, 1.6 M solution in hexane) was added dropwise to a solution of acetonitrile (23.8 mL, 460 mmol) in dry tetrahydrofuran (1000 mL) at –78 °C. After stirring the reaction mixture for 20 min, a solution of 4-bromobenzoyl chloride in dry tetrahydrofuran (50 mL) was added dropwise over 20 min. After 1 h, saturated aqueous ammonium chloride solution was added (200 mL) and the reaction mixture was allowed to warm to room temperature. The product was extracted into ether and washed with 1 N hydrochloric acid (400 mL). The organics were removed in vacuo and the residue was redissolved in ethyl acetate. Ammonium hydroxide was added to give a solid that was filtered, redissolved in ethyl acetate and washed with 2 N hydrochloric acid. The organic layer was washed with brine, dried over sodium sulfate and concentrated in vacuo to give 2-(3-bromobenzoyl)acetonitrile (16.6 g) as a solid.

A mixture of 2-(3-bromobenzoyl)acetonitrile (16.5 g, 73.6 mmol) and *N,N*-diphenylformamidine (14.5 g, 73.6 mmol) in xylene (100 mL) was heated at reflux under a nitrogen atmosphere. After 3 h, the reaction mixture was cooled to room temperature and diluted with ether to give 2-(3-bromobenzoyl)-3-phenylaminoacrylonitrile (17.9 g) as a solid.

A mixture of 4-fluorophenylhydrazine (4.25 g, 33.7 mmol) and 2-(3-bromobenzoyl)-3-phenylaminoacrylonitrile (10.0 g, 30.7 mmol) in ethanol (100 mL) was heated at reflux under a nitrogen atmosphere. After 4 h, the reaction mixture was cooled to room temperature, diluted with hexane to give 5-amino-4-(3-bromobenzoyl)-1-(4-fluorophenyl)pyrazole (9.7 g) as a solid. ¹H NMR (DMSO- d_6) δ 7.18 (s, 2H), 7.41 (t, J = 8.83 Hz, 2H), 7.50 (t, J = 7.83 Hz, 1H), 7.59–7.63 (m, 2H), 7.77–7.10 (m, 3H), 7.84–7.86 (m, 1H). MS (EI/CI) m/z : (M + H) 360.

[5-Amino-1-(2,4-difluorophenyl)-1H-pyrazol-4-yl]-(3-bromophenyl)methanone (17). ¹H NMR (DMSO- d_6) δ 7.27–7.33 (m, 3H), 7.48–7.69 (m, 3H), 7.77–7.86 (m, 4H). MS (EI/CI) m/z : (M + H) 378. Anal. (C₁₆H₁₀BrF₂N₃O) C, H, N.

5-Amino-1-(4-fluorophenyl)-4-[3-iodobenzoyl]pyrazole (18). *n*-Butyllithium (30.5 mL, 76 mmol, 2.5 M solution in hexane) was added dropwise to a cooled (0 °C) solution of diisopropylamine (10.6 mL, 76 mmol) in 10 mL dry tetrahydrofuran. Once addition was complete, the solution was kept at 0 °C for 10 min and was then cooled to –50 °C. This cold LDA solution was then added to a –50 °C solution of acetonitrile (2.37 mL, 45.3 mmol) and ethyl iodobenzoate (10.0 g, 36.2 mmol) in dry tetrahydrofuran (18 mL). Once addition was complete, the reaction was stirred at –50 °C for 3 h and was subsequently warmed to 0 °C. Saturated aqueous ammonium chloride solution was added (20 mL), and the reaction mixture was allowed to warm to room temperature. The product was extracted into ether and washed with 1 N hydrochloric acid (50 mL). The organics were washed with brine (50 mL), dried over magnesium sulfate and then concentrated in vacuo to give a red oil. The oil was purified through a small plug of silica gel using 3:1–2:1 hexanes/ethyl acetate as eluent. Concentration of the column fractions in vacuo gave 2-(3-iodobenzoyl)acetonitrile (8.3 g) as a yellow oil.

A mixture of 2-(3-iodobenzoyl)acetonitrile (36.2 g, 133.5 mmol) and *N,N*-diphenylformamidine (26.2 g, 133.5 mmol) in toluene (200 mL) was heated at reflux under a nitrogen atmosphere. After 8 h, the reaction mixture was cooled to room temperature and diluted with ether (200 mL) to give 2-(3-iodobenzoyl)-3-phenylaminoacrylonitrile (31.2 g) as a solid.

A mixture of 4-fluorophenylhydrazine (26.6 g, 211 mmol) and 2-(3-iodobenzoyl)-3-phenylaminoacrylonitrile (79 g, 211 mmol) in ethanol (400 mL) was heated at reflux under a nitrogen atmosphere. After 30 min, the reaction mixture was cooled to room temperature and then diluted with hexane to give 5-amino-1-(4-fluorophenyl)-4-(3-iodobenzoyl)pyrazole (75.1 g) as a solid. ¹H NMR (DMSO- d_6) δ 7.19 (s, 2H), 7.32–7.44 (m, 3H), 7.59–7.63 (m, 2H), 7.77 (s, 1H), 7.79 (d, J = 7.99 Hz, 1H), 7.96 (d, J = 7.78 Hz, 1H), 8.02 (s, 1H). MS (EI/CI) m/z : (M + H) 407. Anal. (C₁₆H₁₁F₂N₃O) C, H, N.

5-Amino-1-(4-fluorophenyl)-4-[3-(2-morpholin-4-ylethoxy)benzoyl]pyrazole Hydrochloride (21). A mixture of methyl 3-hydroxybenzoate (8.0 g, 56 mmol) and 4-(2-chloroethyl)morpholine hydrochloride (15.7 g, 84 mmol) and potassium carbonate (11.5 g, 83 mmol) in toluene (50 mL) was heated at reflux. After 4 days, the reaction mixture was cooled to room temperature and diluted with ethyl acetate. The organic layer was washed with water and then extracted with dilute hydrochloric acid. The acidic layer was separated, basified with 5 N sodium hydroxide, and the product was extracted into ethyl acetate. The organics were removed in vacuo, and the residue was purified by flash chromatography (elution gradient 3% acetone/methylene chloride) to give methyl 3-(2-morpholin-4-ylethoxy)benzoate (9.0 g) as an oil.

Lithium diisopropylamide (18.8 mL, 37 mmol, 2.0 M solution in heptane/tetrahydrofuran/ethylbenzene) was added dropwise to a solution of acetonitrile (1.58 g, 37 mmol) in dry tetrahydrofuran (50 mL) at –78 °C. After stirring the reaction mixture for 30 min, a solution of methyl 3-(2-morpholin-4-ylethoxy)benzoate in dry tetrahydrofuran (50 mL) was added dropwise over 10 min. After 15 min, water was added and the reaction mixture was allowed to warm to room temperature. The aqueous layer was separated and neutralized with dilute hydrochloric acid to pH 7. The product was extracted into ethyl acetate, washed with water and brine and dried over magnesium sulfate. The organics were removed in vacuo to give 2-[3-(2-morpholin-4-ylethoxy)phenyl]acetonitrile (5.0 g) as an oil which was used in the next step without further purification.

A mixture of 2-[3-(2-morpholin-4-ylethoxy)phenyl]acetonitrile (5.0 g) and *N,N*-diphenylformamidine (5.0 g, 25.5 mmol) in xylene (150 mL) was heated at 100 °C under a nitrogen atmosphere. After 3 h, the reaction mixture was cooled to room temperature and diluted with hexane to give 2-[3-(2-morpholin-4-ylethoxy)benzoyl]-3-phenylaminoacrylonitrile (5.0 g) as a solid.

A mixture of 4-fluorohydrazine (1.0 g, 6.8 mmol) and 2-[3-(2-morpholin-4-ylethoxy)benzoyl]-3-phenylaminoacrylonitrile (2.0 g, 5.3 mmol) in ethanol (30 mL) was heated at reflux under a nitrogen atmosphere. After 6 h, the reaction mixture was cooled to room

temperature and diluted with water. The product was extracted into ethyl acetate, and the organic layer was washed with brine, dried over sodium sulfate and concentrated in vacuo. Purification by flash chromatography (elution gradient: CH₂Cl₂–3% MeOH/CH₂Cl₂) gave 5-amino-1-(4-fluorophenyl)-4-[3-(2-morpholin-4-ylethoxy)-benzoyl]pyrazole which was converted to the hydrochloride salt (0.7 g). ¹H NMR (DMSO-*d*₆) δ 3.12–3.30 (m, 2H), 3.47–3.63 (m, 4H), 3.79–3.91 (m, 2H), 3.93–4.02 (m, 2H), 4.50–4.56 (m, 2H), 7.19 (s, 2H), 7.21–7.26 (m, 1H), 7.32 (s, 1H), 7.37–7.52 (m, 4H), 7.58–7.65 (m, 2H), 7.83 (s, 1H). MS (EI/CI) *m/z*: (M + H) 465. Anal. (C₂₂H₂₃FN₄O₃) C, H, N.

5-Amino-1-(4-fluorophenyl)-1*H*-pyrazole-4-carbothioic Acid *S*-Pyridin-2-yl Ester (24). A mixture of ethyl (ethoxymethylene)-cyanoacetate (26 mL, 154 mmol) and 4-fluorophenyl hydrazine (19.4 g, 154 mmol) in ethanol (125 mL) was heated at reflux. After 16 h, the reaction mixture was cooled to room temperature. The solid was filtered and dried to give 5-amino-4-ethylcarboxy-1-(4-fluorophenyl)pyrazole (28 g) which was suspended in a mixture of 1 N lithium hydroxide (100 mL) and methanol (250 mL). The reaction mixture was heated at reflux. After 16 h, the reaction mixture was filtered through a sinter funnel and the filtrate was acidified with 2 N hydrochloric acid (65 mL). The solid was filtered and dried to give 5-amino-4-carboxy-1-(4-fluorophenyl)pyrazole (21 g).

A mixture of 5-amino-4-carboxy-1-(4-fluorophenyl)pyrazole (15 g, 68 mmol), 2,2'-dipyridinyl disulfide (14.9 g, 68 mmol) and triphenylphosphine (17.8 g, 68 mmol) in acetonitrile (2 L) was stirred at room temperature. After 16 h, the product was filtered and dried to give 5-amino-1-(4-fluorophenyl)-4-(2-pyridylthiocarboxy)pyrazole (14 g).

[5-Amino-1-(4-fluorophenyl)-1*H*-pyrazole-4-yl]-[3-(4-methylpiperazin-1-yl)phenyl]methanone (25). Into an oven dried flask containing magnesium turnings (1.1 g, 45.2 mmol) and tetrahydrofuran (50 mL) was added 1-(3-bromo-phenyl)-4-methylpiperazine (11.6 g, 45.5 mmol), and the reaction mixture was heated at reflux. 5-Amino-1-(4-fluorophenyl)-1*H*-pyrazole-4-carbothioic acid *S*-pyridin-2-yl ester **23** (6.82 g, 12.7 mmol), partially suspended in tetrahydrofuran (75 mL), was added and the mixture was stirred for 18 h at room temperature. The reaction was diluted with ethyl acetate (50 mL) and washed with aqueous ammonium chloride solution and brine and dried over sodium sulfate. The organics were removed in vacuo and the residue was purified by flash chromatography (elution gradient: 3% methanol/dichloromethane) to give [5-amino-1-(4-fluorophenyl)-1*H*-pyrazole-4-yl]-[3-(4-methylpiperazin-1-yl)phenyl]methanone (3.5 g) which was converted to the hydrochloride salt. ¹H NMR (DMSO-*d*₆) δ 2.82 (d, *J* = 4.69 Hz, 3H), 3.14–3.17 (m, 2H), 3.49–3.52 (m, 1H), 3.90–3.94 (m, 1H), 7.23–7.29 (m, 3H), 7.38–7.44 (m, 3H), 7.59–7.63 (m, 2H), 7.79 (s, 1H). MS (EI/CI) *m/z*: (M + H) 443. Anal. (C₂₁H₂₂FN₅O·HCl) C, H, N.

5-Amino-1-(4-fluorophenyl)-4-[3-(2-hydroxyethyl)benzoyl]pyrazole (27). To a solution of 3-bromophenylacetic acid (10 g, 46.5 mmol) in tetrahydrofuran (100 mL) at 0 °C was added diborane (70 mL, 1.0 M solution in tetrahydrofuran). The reaction mixture was allowed to warm to room temperature. After 16 h, the reaction mixture was cooled to 0 °C and water was added dropwise (50 mL). The organic layer was separated, washed with brine, dried over sodium sulfate and concentrated in vacuo. The residue was purified by flash chromatography (elution gradient: 40–60% ethyl acetate/hexane) to give 3-(2-hydroxyethyl)bromobenzene (9.0 g).

To a solution of 3-(2-hydroxyethyl)bromobenzene (4.0 g, 20 mmol) in methylene chloride (100 mL) at 0 °C was added a solution of *tert*-butyldimethylsilyl chloride (3.6 g, 24 mmol), (dimethylamino)pyridine (0.61 g, 5 mmol) and triethylamine (3.6 mL, 25.9 mmol). After 1 h, the reaction mixture was washed with brine and saturated aqueous ammonium chloride solution, dried over sodium sulfate and concentrated in vacuo. The residue was purified by flash chromatography (elution gradient: 0–10% hexane/ethyl acetate) to give 3-(2-*tert*-butyl-dimethylsilyloxyethyl)bromobenzene (6.0 g).

Into an oven dried flask containing magnesium turnings (0.386 g, 15.9 mmol) and tetrahydrofuran (10 mL) was added 3-(2-*tert*-

butyldimethylsilyloxyethyl)bromobenzene (5.0 g, 15.9 mmol), and the reaction mixture was heated at reflux. After 3 h, the reaction mixture was cooled to room temperature, 5-amino-1-(4-fluorophenyl)-4-(2-pyridylthiocarboxy)pyrazole (2.37 g, 7.6 mmol) was added and the stirring was continued for 16 h. The reaction mixture was concentrated in vacuo. The residue was dissolved in ethyl acetate, washed with saturated aqueous ammonium chloride solution and brine and dried over sodium sulfate. The organics were removed in vacuo, and the residue was purified by flash chromatography (elution gradient: 10–30% ethyl acetate/hexane) to give 5-amino-1-(4-fluorophenyl)-4-[3-(2-*tert*-butyldimethylsilyloxyethyl)benzoyl]pyrazole (1.20 g).

To a solution of 5-amino-1-(4-fluorophenyl)-4-[3-(2-*tert*-butyldimethylsilyloxyethyl)benzoyl]pyrazole (1.2 g, 3.0 mmol) in tetrahydrofuran (25 mL) was added tetrabutylammonium fluoride (3.6 mL, 3.6 mmol, 1 M solution in tetrahydrofuran). After 1 h, the reaction mixture was poured into brine, and the product was extracted into ethyl acetate. The organic layer was dried over sodium sulfate, filtered and concentrated in vacuo. The residue was purified by flash chromatography (elution gradient: 40–100% ethyl acetate/hexane) to give 5-amino-1-(4-fluorophenyl)-4-[3-(2-hydroxyethyl)benzoyl]pyrazole (0.8 g). ¹H NMR (DMSO-*d*₆) δ 2.82 (t, *J* = 6.69 Hz, 2H), 3.67 (dd, *J* = 5.27 Hz, *J* = 11.94 Hz, 2H), 4.71 (t, *J* = 5.17 Hz, 1H), 7.16 (s, 2H), 7.37–7.45 (m, 4H), 7.57–7.64 (m, 4H), 7.81 (s, 1H). MS (EI/CI) *m/z*: (M + H) 326. Anal. (C₁₈H₁₆FN₃O₂) C, H, N.

5-Amino-4-[3-(2-aminoethyl)benzoyl]-1-(4-fluorophenyl)pyrazole Hydrochloride (29). To a solution of 5-amino-1-(4-fluorophenyl)-4-[3-(2-hydroxyethyl)benzoyl]pyrazole **27** (0.8 g, 2.5 mmol) in pyridine (10 mL) was added methanesulfonyl chloride (0.29 mL, 3.7 mmol). After 2 h, the reaction mixture was poured into 2 N hydrochloric acid (40 mL), and the product was extracted into ethyl acetate. The organic layer was washed with brine, dried over sodium sulfate, filtered and concentrated in vacuo. The residue was purified by flash chromatography (elution gradient: 40–100% ethyl acetate/hexane) to give methanesulfonic acid 2-{3-[5-amino-1-(4-fluorophenyl)-1*H*-pyrazole-4-carbonyl]phenyl}ethyl ester (0.87 g).

A mixture of 5-amino-1-(4-fluorophenyl)-4-[3-(2-methanesulfonyloxyethyl)benzoyl]pyrazole **28** (0.40 g, 0.99 mmol), sodium azide (0.19 mL, 2.97 mmol) and potassium carbonate (0.41 g, 2.97 mmol) in dimethylformamide (15 mL) was stirred at room temperature. After 16 h, the reaction mixture was poured into brine and the product was extracted into ethyl acetate. The organic layer was dried over sodium sulfate, filtered and concentrated in vacuo. The residue was purified by flash chromatography (elution gradient: 20–50% ethyl acetate/hexane) to give 5-amino-1-(4-fluorophenyl)-4-[3-(2-azidoethyl)benzoyl]pyrazole (0.32 g).

To a solution of 5-amino-1-(4-fluorophenyl)-4-[3-(2-azidoethyl)benzoyl]pyrazole (0.31 g, 0.9 mmol) in tetrahydrofuran (15 mL) was added triphenylphosphine (3.55 g, 1.36 mmol). After 48 h, the reaction mixture concentrated in vacuo. The residue was dissolved in 2 N sodium hydroxide, and the product was extracted into ethyl acetate. The organic layer was dried over sodium sulfate, filtered and concentrated in vacuo. The product was converted to its hydrochloride salt and recrystallized from a mixture of methanol-ethyl acetate to give 5-amino-4-[3-(2-aminoethyl)benzoyl]-1-(4-fluorophenyl)pyrazole hydrochloride salt (0.22 g). ¹H NMR (DMSO-*d*₆) δ 2.50–3.02 (m, 2H), 3.09–3.35 (m, 2H), 7.28 (s, 2H), 7.42 (t, *J* = 8.76 Hz, 2H), 7.50 (d, *J* = 5.50 Hz, 2H), 7.59–7.67 (m, 4H), 7.85 (s, 1H), 8.10 (br, 2H). MS (EI/CI) *m/z*: (M + H) 361. Anal. (C₁₈H₁₇FN₄O₂) C, H, N.

[5-Amino-1-(4-fluorophenyl)-1*H*-pyrazole-4-yl]-[3-[2-(4-methylpiperazin-1-yl)ethyl]phenyl]methanone (30). A mixture of 5-amino-1-(4-fluorophenyl)-4-[3-(2-methanesulfonyloxyethyl)benzoyl]pyrazole **28** (0.22 g, 0.55 mmol), *N*-methylpiperazine (0.18 mL, 1.64 mmol) and potassium carbonate (0.22 g, 1.64 mmol) in dimethylformamide (10 mL) was heated at 70 °C. After 4 h, the reaction mixture was cooled to room temperature and poured into water and the product was extracted into ethyl acetate. The organic layer was washed with brine, dried over sodium sulfate, filtered and concentrated in vacuo. The residue was purified by flash

chromatography (elution gradient: ethyl acetate–20% methanol/ethyl acetate) to afford 5-amino-1-(4-fluorophenyl)-4-[3-[4-methylpiperazin-1-yl]ethyl]pyrazole which was converted to the hydrochloride salt. ¹H NMR (DMSO-*d*₆) δ 2.14 (s, 3H), 2.32–2.57 (m, 10H), 2.83 (t, *J* = 7.48 Hz, 2H), 7.16 (s, 2H), 7.38–7.44 (m, 4H), 7.56–7.64 (m, 4H), 7.82 (s, 1H). MS (EI/CI) *m/z*: (M + H) 499. Anal. (C₂₃H₂₆FN₅O₂·2HCl·0.75H₂O) C, H, N.

3-[5-Amino-1-(4-fluorophenyl)-1H-pyrazole-4-carbonyl]-benzoxonitrile (31). A mixture of 5-amino-4-(3-bromobenzoyl)-1-(4-fluorophenyl)pyrazole **19** (2 g, 5.5 mmol), zinc cyanide (652 mg, 5.5 mmol) and tetrakis(triphenylphosphine)palladium (0) (64 mg, 0.55 mmol) in DMF (2 mL) was heated at 60 °C under argon. After 16 h, the mixture was cooled to room temperature, diluted with ethyl acetate and washed with 2 N NH₄OH. The insoluble material was removed by filtration, and the filtrate was dried over sodium sulfate, concentrated and recrystallized from ethyl acetate/hexane to afford 3-[5-amino-1-(4-fluorophenyl)-1H-pyrazole-4-carbonyl]benzoxonitrile (720 mg). ¹H NMR (DMSO-*d*₆) δ 7.22 (s, 2H), 7.38–7.44 (m, 2H), 7.59–7.63 (m, 2H), 7.74 (t, *J* = 7.76 Hz, 1H), 7.86 (s, 1H), 8.04–8.09 (m, 2H), 8.14–8.15 (m, 1H). MS (EI/CI) *m/z*: (M + H) 306. Anal. (C₁₇H₁₁FN₄O·0.25 H₂O) C, H, N.

4-[5-Amino-1-(4-fluorophenyl)-1H-pyrazole-4-carbonyl]benzoxonitrile (32). ¹H NMR (DMSO-*d*₆) δ 7.24 (br, 2H), 7.38–7.44 (m, 2H), 7.54–7.64 (m, 2H), 7.86 (s, 1H), 7.91 (d, *J* = 8.35 Hz, 2H), 8.00 (d, *J* = 8.52 Hz, 2H), 8.14–8.15 (m, 1H). MS (EI/CI) *m/z*: (M + H) 306. Anal. (C₁₇H₁₁FN₄O·0.1H₂O) C, H, N.

[5-Amino-1-(4-fluorophenyl)-1H-pyrazol-4-yl]-[3-(3-hydroxyprop-1-ynyl)phenyl]methanone (33). A mixture of 5-amino-4-(3-bromobenzoyl)-1-(4-fluorophenyl)pyrazole **19** (1.5 g, 4.2 mmol), propargyl alcohol (0.5 mL, 8.33 mmol), bis(triphenylphosphine)palladium(II) chloride (146 mg, 0.21 mmol) and copper iodide (79 mg, 0.42 mmol) was heated at 70 °C under argon. After 16 h, the mixture was cooled to room temperature, diluted with ethyl acetate and washed with brine. The insoluble material was removed by filtration, and the filtrate was dried over sodium sulfate, concentrated and purified by flash chromatography eluting with 40%–100% ethyl acetate/hexane. The product was recrystallized from ethyl acetate/hexane to afford [5-amino-1-(4-fluorophenyl)-1H-pyrazol-4-yl]-[3-(3-hydroxyprop-1-ynyl)phenyl]methanone (420 mg). ¹H NMR (DMSO-*d*₆) δ 4.33 (d, *J* = 5.97 Hz, 2H), 5.37 (t, *J* = 5.94 Hz, 1H), 7.17 (br, 2H), 7.38–7.44 (m, 2H), 7.50–7.65 (m, 4H), 7.72–7.79 (m, 3H). MS (EI/CI) *m/z*: (M + H) 335. Anal. (C₁₉H₁₄FN₃O₂·C₁₉H₁₄FN₃O₂·0.5H₂O) C, H, N.

[5-Amino-1-(4-fluorophenyl)-1H-pyrazol-4-yl]-[3-(3-(dimethylamino)prop-1-ynyl)phenyl]methanone (34). ¹H NMR (DMSO-*d*₆) δ: 2.87 (s, 6 H), 4.34 (s, 2 H), 7.21 (s, 2 H), 7.42 (t, *J* = 8.82 Hz, 2 H), 7.58–7.64 (m, 3 H), 7.75–7.87 (m, 4 H). MS (EI/CI) *m/z*: (M + H) 362. Anal. (C₂₁H₁₉FN₄O·HCl) C, H, N.

[5-Amino-1-(4-fluorophenyl)-1H-pyrazol-4-yl]-[3-[3-(4-methylpiperazin-1-yl)prop-1-ynyl]phenyl]methanone (35). ¹H NMR (DMSO-*d*₆) δ 2.85 (s, 3H), 3.32 (br, 4H), 3.64 (br, 4H), 4.21 (s, 2H), 7.41 (t, *J* = 8.83 Hz, 2H), 7.59–7.76 (m, 3H), 7.77–7.84 (m, 4H). MS (EI/CI) *m/z*: (M + H) 417. Anal. (C₂₄H₂₄FN₅O·2HCl) C, H, N.

[5-Amino-1-(4-fluorophenyl)-1H-pyrazol-4-yl]-[3-(3-piperidin-1-ylprop-1-ynyl)phenyl]methanone (36). ¹H NMR (DMSO-*d*₆) δ 1.82 (br, 6H), 3.02 (br, 2H), 3.45 (br, 2H), 4.31 (s, 2H), 7.20 (s, 2H), 7.41 (t, *J* = 8.82 Hz, 2H), 7.57–7.64 (m, 3H), 7.74–7.86 (m, 4H). MS (EI/CI) *m/z*: (M + H) 439. Anal. (C₂₄H₂₃FN₄O·HCl) C, H, N.

5-Amino-1-(4-fluorophenyl)-1H-pyrazol-4-yl]-[3-(3-morpholin-4-ylprop-1-ynyl)phenyl]methanone (37). ¹H NMR (DMSO-*d*₆) δ 3.22 (br, 2H), 3.41 (br, 2H), 3.92 (br, 2H), 4.37 (s, 2H), 7.20 (s, 2H), 7.38–7.44 (m, 2H), 7.58–7.63 (m, 3H), 7.74–7.87 (m, 4H). MS (EI/CI) *m/z*: (M + H) 404. Anal. (C₂₃H₂₁FN₄O₂·HCl) C, H, N.

[5-Amino-1-(4-fluorophenyl)-1H-pyrazol-4-yl]-[4-(3-morpholin-4-ylprop-1-ynyl)phenyl]methanone (38). ¹H NMR (DMSO-*d*₆) δ 3.49–2.56 (m, 4H), 3.57 (s, 2H), 3.63 (t, *J* = 4.64 Hz, 4H), 7.18 (br, 2H), 7.38–7.44 (m, 2H), 7.57–7.63 (m, 2H), 7.77 (d, *J*

= 8.31 Hz, 2H), 7.82 (s, 1H). MS (EI/CI) *m/z*: (M + H) 404. Anal. (C₂₃H₂₁FN₄O₂) C, H, N.

[5-Amino-1-(4-fluorophenyl)-1H-pyrazol-4-yl]-[3-(3-morpholin-4-ylpropyl)phenyl]methanone (39). ¹H NMR (DMSO-*d*₆) δ 2.09 (m, 2H), 2.76 (t, *J* = 7.68 Hz, 2H), 3.02–3.09 (m, 4 H), 3.77–3.95 (m, 4H), 7.16 (br, 2H), 7.39–7.49 (m, 2H), 7.59–7.63 (m, 2H), 7.81 (s, 2H). MS (EI/CI) *m/z*: (M + H) 408. Anal. (C₂₃H₂₅FN₄O₂·HCl) C, H, N.

[5-Amino-1-(4-fluorophenyl)-1H-pyrazol-4-yl]-[4-(3-morpholin-4-ylpropyl)phenyl]methanone (40). ¹H NMR (DMSO-*d*₆) δ 2.09 (m, 2H), 2.74 (t, *J* = 7.66 Hz, 2H), 3.02–3.09 (m, 4 H), 3.40–3.50 (m, 4H), 3.83–3.96 (m, 4H), 7.15 (br, 2H), 7.38–7.44 (m, 4 H), 7.59–7.64 (m, 2H), 7.74 (d, *J* = 8.11 Hz, 2H) 7.81 (s, 1H). MS (EI/CI) *m/z*: (M + H) 408. Anal. (C₂₃H₂₅FN₄O₂·HCl) C, H, N.

5-Amino-4-[3-(2-aminosulfonyl)ethyl]benzoyl]-1-(4-fluorophenyl)pyrazole (45). A mixture of 5-amino-4-(3-bromobenzoyl)-1-(4-fluorophenyl)pyrazole (1.5 g, 4.14 mmol), vinylsulfonamide (1.33 g, 12.4 mmol), bis(triphenylphosphine)palladium chloride (0.3 g, 0.42 mmol) and triethylamine (6 mL, 43 mmol) in dimethylformamide (18 mL) was heated at 100 °C under argon. After 16 h, the reaction mixture was cooled to room temperature and poured into 1 N hydrochloric acid. The product was extracted into ethyl acetate, washed with brine, dried over sodium sulfate and filtered. The organic layer was removed in vacuo, and the residue was purified by flash chromatography (elution gradient: 40–80% ethyl acetate/hexane) to give 5-amino-4-[3-(2-aminosulfonyl)ethyl]benzoyl]-1-(4-fluorophenyl)pyrazole which was recrystallized from a mixture of methanol/ethyl acetate/hexane to give 0.78 g of the desired product.

A mixture of 5-amino-4-[3-(2-aminosulfonyl)ethyl]benzoyl]-1-(4-fluorophenyl)pyrazole (2.1 g, 5.43 mmol) and palladium hydroxide (0.6 g) in methanol (150 mL) was shaken in a Parr apparatus under hydrogen atmosphere at 50 psi. After 4 days, the reaction mixture was filtered through Celite, and the filtrate was concentrated. The residue was purified by flash chromatography (elution gradient: 40–100% ethyl acetate/hexane) to give a crude product which was recrystallized from methanol/ethyl acetate/hexane to give 5-amino-4-[3-(2-aminosulfonyl)ethyl]benzoyl]-1-(4-fluorophenyl)pyrazole (0.95 g) as a solid. ¹H NMR (DMSO-*d*₆) δ 3.09–3.15 (m, 2H), 3.32–3.37 (m, 2H), 6.90 (s, 2H), 7.17 (s, 2H), 7.38–7.50 (m, 4H), 7.59–7.65 (m, 4H), 7.85 (s, 1H). MS (EI/CI) *m/z*: (M + H) 388. Anal. (C₁₈H₁₇FN₃O₃S) C, H, N.

[5-Amino-1-(4-fluorophenyl)-1H-pyrazol-4-yl]-[3-(2-methanesulfonyl)ethyl]phenyl]methanone (46). ¹H NMR (CDCl₃) δ 2.89 (s, 3H), 3.24–3.39 (m, 4H), 6.05 (s, 2H), 7.22–7.28 (m, 2H), 7.42–7.58 (m, 4H), 7.68–7.74 (m, 2H), 7.76 (s, 1H). MS (EI/CI) *m/z*: (M + H) 388. Anal. (C₁₉H₁₈FN₃O₃S·0.45 H₂O) C, H, N.

[5-Amino-1-(4-fluorophenyl)-1H-pyrazol-4-yl]-[3-[2-(1-hydroxycyclopentyl)ethyl]phenyl]methanone (47). ¹H NMR (CDCl₃) δ 1.59–1.96 (m, 10 H), 2.83–2.88 (m, 2H), 6.07 (s, 2H), 7.20–7.27 (m, 2H), 7.40 (d, *J* = 5.01 Hz, 2H), 7.52–7.58 (m, 2H), 7.60–7.65 (m, 2H), 7.78 (s, 1H). MS (EI/CI) *m/z*: (M + H) 394. Anal. (C₂₃H₂₄FN₃O₂) C, H, N.

[5-Amino-1-(4-fluorophenyl)-1H-pyrazol-4-yl]-[3-(3-hydroxy-3-methylbutyl)phenyl]methanone (48). ¹H NMR (CDCl₃) δ 1.16 (s, 6 H), 1.66–1.72 (m, 2H), 2.70–2.76 (m, 2H), 4.30 (s, 1 H), 7.16 (s, 2H), 7.38–7.44 (m, 4H), 7.56–7.65 (m, 4H), 7.91 (s, 1H). MS (EI/CI) *m/z*: (M + H) 368. Anal. (C₂₁H₂₂FN₃O₂) C, H, N.

[5-Amino-1-(4-fluorophenyl)-1H-pyrazol-4-yl]-[3-(1,2-dihydroxyethyl)phenyl]methanone (50). To a solution of 5-amino-1-(4-fluorophenyl)-4-[3-iodobenzoyl]pyrazole (15.0 g, 36.85 mmol) in DMF (150 mL) were added vinyltributyltin (12.85 g, 40.54 mmol) and tetrakis(triphenylphosphine)palladium(0) (2.13 g, 1.84 mmol). The reaction was degassed with argon and then warmed to 100 °C under argon. After 18 h the reaction was cooled to room temperature and then poured into water (500 mL). The product was extracted into 1:1 ether/ethyl acetate, and the combined organic extracts were washed with water and brine and dried over magnesium sulfate. Concentration in vacuo gave an oil which was purified by flash column chromatography using 5:1–4:1 hexane/

ethyl acetate to remove the byproducts and 3:1 to 2:1 hexane/ethyl acetate to elute [5-amino-1-(4-fluorophenyl)-1*H*-pyrazol-4-yl]-(3-vinylphenyl)methanone (10.06 g).

To a suspension of [5-amino-1-(4-fluorophenyl)-1*H*-pyrazol-4-yl]-(3-vinylphenyl)methanone (8.0 g, 24.92 mmol) in *tert*-butyl alcohol (90 mL) was added *N*-methylmorpholine *N*-oxide (3.2 g, 27.41 mmol) in water (90 mL). To this slurry at room temperature was then added osmium tetroxide (9.375 mL, 0.747 mmol, 2.5% in *tert*-butyl alcohol). After 18 h, the reaction was complete and homogeneous. The product was extracted into ethyl acetate, and the combined organic extracts were washed with water and brine and dried over magnesium sulfate. Concentration in vacuo gave a brown oil which was purified by flash column chromatography using 1:1 hexane/ethyl acetate as eluent. The product eluted with 100% ethyl acetate to afford [5-amino-1-(4-fluorophenyl)-1*H*-pyrazol-4-yl]-(3-(1,2-dihydroxyethyl)phenyl)methanone (4.96 g). ¹H NMR (DMSO-*d*₆) δ 3.44–3.99 (m, 2H), 4.62–4.68 (m, 1H), 4.80 (t, *J* = 5.78 Hz, 1H), 5.40 (d, *J* = 4.33 Hz, 1H), 7.16 (s, 2H), 7.38–7.65 (m, 7H), 7.77 (s, 1H), 7.81 (s, 1H). MS (EI/CI) *m/z*: (M + H) 342. Anal. (C₁₈H₁₆FN₃O₃) C, H, N.

Synthesis of 5-Amino-1-(4-fluorophenyl)-4-[3-(pyridin-3-yl)-benzoyl]pyrazole (51). A mixture of 5-amino-4-(3-bromobenzoyl)-1-(4-fluorophenyl)pyrazole (0.9 g, 2.5 mmol), pyridine-3-boronic acid, 1,3-propanediol cyclic ester (0.5 g, 3 mmol), potassium phosphate (0.8 g, 3.73 mmol) and tetrakis(triphenylphosphine)palladium (0.3 g, 0.25 mmol) in dioxane (20 mL) was heated at 85 °C under argon. After 16 h, the reaction mixture was cooled to room temperature and poured into brine. The product was extracted into ethyl acetate, dried over sodium sulfate and filtered. The organic layer was removed in vacuo, and the residue was purified by flash chromatography (elution gradient: 40–80% ethyl acetate/hexane) to give 5-amino-1-(4-fluorophenyl)-4-[3-(pyridin-3-yl)benzoyl]pyrazole (0.50 g) which was recrystallized from ethyl acetate. ¹H NMR (DMSO-*d*₆) δ 7.25 (br, 2H), 7.39–7.45 (m, 2H), 7.60–7.65 (m, 2H), 7.75 (t, *J* = 7.71 Hz, 1H), 7.90 (d, *J* = 7.75 Hz, 1H), 7.95 (s, 1H), 8.08–8.10 (m, 2H), 8.19 (s, 1H), 8.86–8.91 (m, 2H), 9.33 (s, 1H). MS (EI/CI) *m/z*: (M + H) 359. Anal. (C₂₁H₁₅FN₄O·HCl) C, H, N.

[5-Amino-1-(4-fluorophenyl)-1*H*-pyrazol-4-yl]-(4-pyridin-3-ylphenyl)methanone (52). ¹H NMR (DMSO-*d*₆) δ 7.25 (br, 2H), 7.39–7.45 (m, 2H), 7.60–7.65 (m, 2H), 7.86 (s, 1H), 7.95 (d, *J* = 6.51 Hz, 2H), 8.03–8.09 (m, 3H), 8.82 (d, *J* = 4.68 Hz, 1H), 8.90 (d, *J* = 5.48 Hz, 1H), 9.29 (d, *J* = 2.05 Hz, 1H). MS (EI/CI) *m/z*: (M + H) 359. Anal. (C₂₁H₁₅FN₄O·HCl) C, H, N.

[5-Amino-1-(4-fluorophenyl)-1*H*-pyrazol-4-yl]-(3-pyridin-4-ylphenyl)methanone (53). ¹H NMR (DMSO-*d*₆) δ 7.25 (br, 2H), 7.39–7.45 (m, 2H), 7.60–7.65 (m, 2H), 7.79 (t, *J* = 7.74 Hz, 1H), 7.92 (s, 1H), 7.99 (d, *J* = 7.79 Hz, 1H), 8.21 (d, *J* = 7.78 Hz, 1H), 8.28 (s, 1H), 8.45 (d, *J* = 6.73 Hz, 2H), 8.98 (d, *J* = 6.71 Hz, 2H). MS (EI/CI) *m/z*: (M + H) 359. Anal. (C₂₁H₁₅FN₄O·HCl·0.15H₂O) C, H, N.

[5-Amino-1-(2,4-difluorophenyl)-1*H*-pyrazol-4-yl]-(3-pyridin-4-ylphenyl)methanone (54). ¹H NMR (DMSO-*d*₆) δ 7.28–7.34 (m, 3H), 7.56–7.66 (m, 2H), 7.79 (t, *J* = 7.74 Hz, 1H), 7.92 (s, 1H), 7.99 (d, *J* = 7.79 Hz, 1H), 8.21 (d, *J* = 7.78 Hz, 1H), 8.28 (s, 1H), 8.45 (d, *J* = 6.73 Hz, 2H), 8.98 (d, *J* = 6.71 Hz, 2H). MS (EI/CI) *m/z*: (M + H) 377. Anal. (C₂₁H₁₄F₂N₄O·HCl·0.25 H₂O) C, H, N.

[5-Amino-1-(2,4-difluorophenyl)-1*H*-pyrazol-4-yl]-(3-pyridin-3-ylphenyl)methanone (55). ¹H NMR (DMSO-*d*₆) δ 7.29–7.34 (m, 1H), 7.52–7.69 (m, 2H), 7.78 (t, *J* = 7.73 Hz, 1H), 7.92 (s, 1H), 7.94 (s, 1H), 8.06–8.14 (m, 2H), 8.17 (s, 1H), 8.88–8.91 (m, 2H), 9.30 (s, 1H). MS (EI/CI) *m/z*: (M + H) 377. Anal. (C₂₁H₁₄F₂N₄O·HCl) C, H, N.

[5-Amino-1-(2,4-difluorophenyl)-1*H*-pyrazol-4-yl]-(3-(1-oxypyridin-3-yl)phenyl)methanone (56). To a suspension of [5-amino-1-(2,4-difluorophenyl)-1*H*-pyrazol-4-yl]-(3-pyridin-3-ylphenyl)methanone **56** (4.4 g, 11.7 mmol) in dichloromethane (100 mL) at room temperature under nitrogen was added 3-chloroperoxybenzoic acid (7.8 g, 45.2 mmol). The mixture turned reddish-brown and became homogeneous. After 18 h the mixture was poured into 10%

aqueous Na₂SO₃ and extracted into dichloromethane, dried over sodium sulfate, concentrated in vacuo and purified by flash chromatography eluting with 100% ethyl acetate and then 3% methanol/ethyl acetate to give [5-amino-1-(2,4-difluorophenyl)-1*H*-pyrazol-4-yl]-(3-(1-oxypyridin-3-yl)phenyl)methanone which was recrystallized from methanol (1.3 g). ¹H NMR (DMSO-*d*₆) δ 7.27–7.34 (m, 1H), 7.50–7.56 (m, 5H), 7.84 (d, *J* = 6.43 Hz, 1H), 7.93–7.97 (m, 2H), 8.02 (s, 1H), 8.26 (d, *J* = 4.68 Hz, 1H), 8.68 (s, 1H). MS (EI/CI) *m/z*: (M + H) 392. Anal. (C₂₁H₁₄F₂N₄O₂·0.2H₂O) C, H, N.

[5-Amino-1-(4-fluorophenyl)-1*H*-pyrazol-4-yl]-(3-(1,2-dihydroxy-1-hydroxymethylethyl)phenyl)methanone (58). To a solution of 5-amino-1-(4-fluorophenyl)-4-(3-iodobenzoyl)pyrazole (1.0 g, 2.46 mmol) in DMF (10 mL) were added potassium carbonate anhydrous (733 mg, 7.37 mmol), diboron pinacol ester (0.686 g, 2.70 mmol) and dichloro[1,1'-bis(diphenylphosphino)ferrocene]palladium(II) dichloromethane adduct (0.20 g, 0.246 mmol). The solution was degassed with argon and warmed to 80 °C for 2 h. The reaction was then cooled to room temperature and dichloro[1,1'-bis(diphenylphosphino)ferrocene]palladium(II) dichloromethane adduct (200 mg, 0.246 mmol) was added along with (2-bromoallyloxymethyl)benzene (0.613 g, 2.70 mmol) and sodium carbonate (1.3 g, 12.3 mmol) in water (6 mL). The reaction was again degassed and warmed back to 80 °C. After 18 h, the reaction was cooled to room temperature and was poured into water (100 mL), and the product was extracted into ethyl acetate. The combined ethyl acetate extracts were washed with brine and dried over magnesium sulfate. Concentration in vacuo gave a brown oil which was purified by flash column chromatography using 4:1–2:1 hexane/ethyl acetate to yield [5-amino-1-(4-fluorophenyl)-1*H*-pyrazol-4-yl]-(3-(1-benzyloxymethylvinyl)phenyl)methanone (380 mg).

To a solution of [5-amino-1-(4-fluorophenyl)-1*H*-pyrazol-4-yl]-(3-(1-benzyloxymethylvinyl)phenyl)methanone **57** (0.38 g, 0.889 mmol) in *tert*-butyl alcohol were added *N*-methylmorpholine *N*-oxide (0.114 g, 0.978 mmol) and water (3 mL). To this solution was then added osmium tetroxide (0.56 mL, 0.04 mmol). The reaction was stirred at room temperature for 8 h. The reaction was poured into ethyl acetate (25 mL) and washed with brine. The organic layer was separated and dried over magnesium sulfate. Concentration in vacuo gave a brown oil which was purified by flash column chromatography using 1:1 hexane/ethyl acetate to remove impurities and 4:1 ethyl acetate/hexane to elute [5-amino-1-(4-fluorophenyl)-1*H*-pyrazol-4-yl]-(3-(2-benzyloxy-1-hydroxy-1-hydroxymethylethyl)phenyl)methanone (73 mg).

To a solution of [5-amino-1-(4-fluorophenyl)-1*H*-pyrazol-4-yl]-(3-(2-benzyloxy-1-hydroxy-1-hydroxymethylethyl)phenyl)methanone (320 mg, 0.694 mmol) in ethanol (25 mL) was added 10% Pd/C (100 mg). The reaction was stirred at room temperature under hydrogen. After 72 h, the palladium was removed by filtration through Celite. The filtrate was concentrated to an oil and purified by flash chromatography using 2:1 ethyl acetate/hexane–100% ethyl acetate as eluent to yield [5-amino-1-(4-fluorophenyl)-1*H*-pyrazol-4-yl]-(3-(1,2-dihydroxy-1-hydroxymethylethyl)phenyl)methanone (152 mg). ¹H NMR (DMSO-*d*₆) δ 3.78 (d, *J* = 11.4 Hz, 2H), 3.94 (d, *J* = 11.4 Hz, 2H), 6.31 (s, 2H), 7.21–7.26 (m, 2H), 7.45–7.58 (m, 3H), 7.68–7.73 (m, 2H), 7.80 (s, 1H), 7.98 (s, 1H). MS (EI/CI) *m/z*: (M + H) 372. Anal. (C₁₉H₁₈FN₃O₄·0.7 H₂O) C, H, N.

[5-Amino-1-(4-fluorophenyl)-1*H*-pyrazol-4-yl]-(3-(2-piperidin-1-yl-ethoxy)phenyl)methanone (61). [5-Amino-1-(4-fluorophenyl)-1*H*-pyrazol-4-yl]-(3-hydroxyphenyl)methanone (1.5 g, 5.05 mmol) was combined with toluene (50 mL). 2-Bromoethanol (1.79 mL, 25.23 mmol) was added, and the mixture was cooled to 0 °C. Triphenylphosphine (5.425 g, 20.69 mmol) and diethyl azodicarboxylate (3.26 mL, 20.69 mmol) were then added. The reaction was allowed to warm to room temperature. After stirring for 16 h, the reaction was quenched with a saturated aqueous ammonium chloride solution, extracted with ethyl acetate, dried over magnesium sulfate, filtered and concentrated in vacuo. The product was purified by column chromatography on silica gel using 40:1 CH₂Cl₂/MeOH

and then stirred with ether for 20 min, filtered and dried to give 0.785 g of [5-amino-1-(4-fluorophenyl)-1H-pyrazol-4-yl]-(3-bromophenyl)methanone **60**.

[5-Amino-1-(4-fluorophenyl)-1H-pyrazol-4-yl]- (3-bromophenyl)methanone **60** (0.6 g, 1.48 mmol) was combined with piperidine (1.47 mL, 14.8 mmol) and ethanol (10 mL) and heated at reflux for 16 h. The reaction mixture was concentrated in vacuo. The resulting residue was partitioned between a saturated aqueous sodium hydrogen carbonate solution and ethyl acetate. The organic extracts were dried over magnesium sulfate, filtered, concentrated under vacuum and purified by column chromatography on silica gel using 16:1 CH₂Cl₂/MeOH. Dissolving the product in ethyl acetate then adding hydrochloric acid (1.0 M, 1.0 equivalent) formed the hydrochloric salt which was filtered and dried to give 0.413 g of [5-amino-1-(4-fluorophenyl)-1H-pyrazol-4-yl]-[3-(2-piperidin-1-yl-ethoxy)phenyl]methanone. ¹H NMR (DMSO-*d*₆) δ 1.39 (m, 1H), 1.66–1.98 (m, 5 H), 3.00 (m, 2H), 3.49 (m, 4H), 4.49 (t, *J* = 4.92 Hz, 2H), 7.17–7.23 (m, 3H), 7.29 (m, 1 H), 7.38–7.51 (m, 4H), 7.57–7.62 (m, 2H), 7.81 (m, 1H). MS (EI/CI) *m/z*: (M + H) 409. Anal. (C₂₃H₂₅FN₄O₂) C, H, N.

5-Amino-1-(4-fluorophenyl)-4-[3-{2(R), 3-dihydroxypropoxy}benzoyl]pyrazole (62). To a solution of 5-amino-4-(3-hydroxybenzoyl)-1-(4-fluorophenyl)pyrazole (8.0 g, 26.9 mmol) in 30 mL dry dimethylformamide was added D-α,β-isopropylidene-glycerol γ-tosylate (11.3 g, 39.5 mmol) followed by anhydrous potassium carbonate (11.13 g, 80.7 mmol). The reaction was warmed to 80 °C under argon. After 24 h, the reaction was cooled to room temperature and diluted with distilled water (100 mL), and the product was extracted into ethyl acetate. The combined organics were washed with brine, dried over magnesium sulfate and then concentrated in vacuo to a brown oil. The oil was purified by flash column chromatography on silica gel using 2:1–1:1 hexanes/ethyl acetate as eluent. Concentration of the column fractions in vacuo gave 9.32 g of the desired acetal.

To a solution of the acetal formed above (17.42 g, 42 mmol) in methanol (80 mL) were added distilled water (20 mL) and *p*-toluenesulfonic acid monohydrate (500 mg). The solution was warmed to 50 °C under an argon atmosphere. After 6 h, the reaction mixture was cooled to room temperature and concentrated in vacuo to a yellow oil. The oil was redissolved in ethyl acetate and 5% sodium bicarbonate solution (50 mL). The organic layer was separated, dried over magnesium sulfate and concentrated in vacuo, and the desired diol precipitated out of solution to give 13 g of a white solid. The solid had a small amount of impurity and was thus suspended in 150 mL 1:1 hexanes/ethyl acetate and stirred for 1 h. Filtration of the undissolved solid gave pure diol (12.03 g). ¹H NMR (DMSO-*d*₆) δ 3.47 (t, *J* = 5.69 Hz, 2H), 3.78–3.87 (m, 1H), 3.92–3.97 (m, 1H), 4.07–4.12 (m, 1H), 4.72 (t, *J* = 5.71 Hz, 1H), 5.02 (d, *J* = 5.13 Hz, 1H), 7.14–7.18 (m, 3H), 7.25–7.26 (m, 1H), 7.32–7.47 (m, 4H), 7.59–7.66 (m, 2H), 7.81 (s, 1H). MS (EI/CI) *m/z*: (M + H) 372. Anal. (C₁₉H₁₈FN₃O₄·0.25H₂O) C, H, N.

5-Amino-1-(4-fluorophenyl)-4-[3-{2(S),3-dihydroxypropoxy}benzoyl]pyrazole (63). ¹H NMR (DMSO-*d*₆) δ 3.47 (t, *J* = 5.68 Hz, 2H), 3.78–3.85 (m, 1H), 3.92–3.97 (m, 1H), 4.07–4.12 (m, 1H), 4.72 (t, *J* = 5.71 Hz, 1H), 5.02 (d, *J* = 5.12 Hz, 1H), 7.14–7.18 (m, 3H), 7.25–7.26 (m, 1H), 7.32–7.47 (m, 4H), 7.59–7.66 (m, 2H), 7.81 (s, 1H). MS (EI/CI) *m/z*: (M + H) 372. Anal. (C₁₉H₁₈FN₃O₄) C, H, N.

Crystallization and Structure Determination. Crystallization and structure determination of p38 MAP kinase with compound **55** was performed as reported previously.⁴ Crystals were obtained in the space group *P*2₁2₁2₁ with cell dimensions of *a* = 45.3 Å, *b* = 86.5 Å, *c* = 124.1 Å. X-ray diffraction data were collected at the Advance Light Source, Lawrence Berkeley National Laboratory, and data between 36.6 and 1.75 Å (41 760 unique reflections) were reduced using HKL2000.¹⁵ The structure was refined using CNS¹⁶ to a final *R*_{factor} = 20.1 and *R*_{free} = 24.1, including 293 water molecules in the final structure. Overall the protein structure has good geometry, with 89.7% of the residues in the core region of a Ramachandran plot, 10% in the allowed region and 0.3% in the

generously allowed region. Details of the data collection and statistics and structure refinement are reported along with the structure coordinates, which have been deposited in the Protein Data Bank.¹⁷ Pictures of the p38 MAP kinase structure (Figure 1) were made using PyMOL.¹⁸

Biological Methods. p38 MAP Kinase Inhibition. HTS Assay. HTS was performed using a Zymark robotic system and a 96-well, radioactive filtration binding format. The enzyme was preincubated with test compounds (40 μM) for 10 min. at 30 °C, following which the reaction was initiated by adding [³³P] ATP (250 μM) and myelin basic protein (150 μM). Following an additional incubation for 20 min at 30 °C the reaction was terminated, and the radiolabeled product was captured on nitrocellulose filtration plate, washed and counted for radioactivity. Compounds which displayed >40% inhibition of the enzyme activity were retested at multiple concentrations.

In Vitro Assay. Inhibition of human recombinant active p38α [5 nM] was tested by measuring the incorporation of ³³P from γ-[³³P] ATP [50 μM, 1 μCi] into myelin basic protein (MBP) (35 μM). The assay was performed in a 96-well microtiter plate. In 40 μL reaction volume, 26 μL diluted p38α (5 nM) in assay dilution buffer (ADB) (20 mM MOPS pH 7.4, 40 mM MgCl₂, 1 mM DTT, 25 mM β-glycerol phosphate, 5 mM EGTA, 1 mM sodium orthovanadate) were preincubated at room temperature for 10 min with 4 μL test compounds (0–100 μM), dissolved in dimethyl sulfoxide (DMSO) (10%). The kinase reaction was initiated by the addition of 10 μL assay mix, containing ADB and γ-[³³P] ATP (50 μM, 1 μCi) and MBP (35 μM). After 30 min incubation at 30 °C, the reactions were terminated by transferring 25 μL reaction samples onto a prewetted phosphocellulose filter plate (Millipore) containing 200 μL 0.75% phosphoric acid (H₃PO₄). The plate membranes were washed three times with 200 μL 0.75% H₃PO₄ for the removal of the free radionucleotide. 50 μL Microscint-20 scintillant (Packard) was added to each well; the plate was sealed with a plastic film and counted in a Packard Topcount microplate scintillation counter. The 50% inhibitory value was calculated by fitting the data to the equation:

$$\text{fractional activity} = 1/[1/IC_{50} + 1]$$

Induction of TNF Biosynthesis. THP1 cells were suspended in culture medium [RPMI (Gibco-BRL, Gaithersburg, MD) containing 15% fetal bovine serum, 0.02 mM 2-mercaptoethanol], at a concentration of 2.5 × 10⁶ cells/mL and then plated in a 96-well plate (0.2 mL aliquots in each well). Test compounds were dissolved in DMSO and then diluted with the culture medium such that the final DMSO concentration was 5%. Twenty-five microliter aliquots of test solution or medium with DMSO (control) were added to each well. The cells were incubated for 30 min, at 37 °C. LPS (Sigma, St. Louis, MO) was added to the wells at a final concentration of 0.5 μg/mL, and cells were incubated for an additional 2 h. At the end of the incubation period, culture supernatants were collected and the amount of TNF-α present was determined by a specific trapping ELISA assay using two anti-TNF-α antibodies (2TNF-H22 and 2TNF-H34) as described.¹⁹

Inhibition of TNFα and IL-1β Biosynthesis in LPS-Stimulated Peripheral Blood Mononuclear Cells. Blood was collected from healthy volunteers (drug-free for two weeks) into vacutainers (Becton Dickinson, Mountainview, CA) containing 19 units/mL sodium heparin. Peripheral blood mononuclear cells (PBMC) were separated using a Histopaque-1077 gradient (Sigma; H-8889). Briefly, whole blood was diluted 1:1 in Dulbecco's phosphate-buffered saline (Gibco; #14190-136) and layered onto the histopaque solution followed by centrifugation at 400g for 20 min at room temperature. Cells were collected and washed once in cold PBS followed by red cell lysis with lysing media (Sigma #R-7757, Lot #46H2373). A final cell suspension was prepared at 2 × 10⁶ per mL in RPMI 1640 (Gibco BRL, #11875-085), 10% FBS, 2 mM l-glutamine, 5.5 × 10⁻⁵ M β-mercaptoethanol. Dilutions of test compounds were redispensed in 25 μL aliquots (before addition of cells) into round-bottom 96-well plates (U bottom TC

plate; Costar #3799). The starting concentration was 100 μM in 5% DMSO and 6 half log serial dilutions were made. After the addition of 200 μL cell suspension and 25 μL of 5 $\mu\text{g}/\text{mL}$ lipopolysaccharide (LPS, *E. coli*; 0127; B8; Cat. No. L3129, Sigma Chemical Co., St. Louis, MO) in medium, the final DMSO concentration was 0.5%. Aliquots of test compounds were diluted an additional 10-fold, and the final LPS concentration was 500 ng/mL. PBMC suspension (200 μL per sample) was preincubated with the diluted compound for 30 min at 37 °C followed by addition of 25 μL of LPS dissolved in RPMI (Gibco BRL, #11875-085) to produce a final LPS concentration of 0.5 $\mu\text{g}/\text{mL}$. Negative control wells received RPMI alone. Plates were incubated for 2 or 5 h at 37 °C in a 5% CO_2 atmosphere for determination of TNF α or IL-1 β , respectively, followed by centrifugation at 150g for 10 min. Supernatants were collected from each sample and stored in polypropylene plates at 4 °C. TNF- α and IL-1 β were determined by Elisa (Antibody Solutions, Palo Alto, CA) following the manufacturer's instructions. Optical density of each sample was read at 450 nm with a reference of 650 nm. Cytokine concentrations were determined from a standard curve using Molecular Devices SoftMax Pro. The percent inhibition was calculated for each concentration tested and an IC₅₀ curve was constructed using Xlfit software.

Systemic LPS and TNF- α Challenge. All animal procedures were approved by the Institutional Animal Care and Use Committee of Roche Palo Alto. Female Hanover–Wistar rats (100–130 g) were purchased from Charles River Laboratories (Hollister, CA). Animals were randomly segregated into groups (8 per group) and treated with LPS (Sigma, St Louis, MO; 50 $\mu\text{g}/\text{kg}$ intraperitoneally in 0.9% saline) or TNF- α (R&D Systems, Minneapolis, MN; 5 $\mu\text{g}/\text{kg}$ intraperitoneally in 0.9% saline). Animals were treated with vehicle or compound **63** by oral gavage 30 min prior to LPS or TNF- α challenge. Animals were euthanized 90 min after the challenge by CO_2 inhalation and serum harvested. TNF- α and IL-6 levels were measured in serum samples by ELISA (Biosource International, Camarillo, CA) according to the manufacturer's instructions.

Rat Adjuvant Arthritis (AI). Female Lewis rats (120–150 g) from Charles River Laboratories were randomized and immunized with heat killed *Mycobacterium butyricum* (Difco Laboratories, Detroit, MI) in light mineral oil (Sigma; 5 mg/ml) by intradermal injection (0.1 mL) into the tail on day 0. Vehicle (PEG 400) and compound **63** were subcutaneously delivered from day one onward by osmotic minipump (Alza; Mountain View, CA). Two minipumps were implanted to each rat and replaced on day eight. Plasma samples were collected on days three and fourteen. Animals were euthanized on day fourteen and hind paw weights recorded in addition to clinical scores.

Rat Pharmacokinetic Study. Female Wistar/Han (CRL:WI) Rats (Charles River, Hollister, CA) weighing between 180 and 220 g were used. Animals were allowed free access to a standard laboratory chow and tap water and were housed in a constant temperature-humidity environment. Three rats per dose regime were administered either single 10-mg/kg iv bolus doses (50% cyclo-dextran/water) or single 10-mg/kg oral suspension doses prepared in aqueous vehicle containing 0.9% NaCl, 0.5% sodium carboxymethyl cellulose, 0.4% polysorbate 80 and 0.9% benzyl alcohol. Blood was collected from each rat anesthetized with CO_2/O_2 (60:40) via the orbital sinus or cardiac puncture at 1, 3, 6, 8 and 24 h after dosing. Plasma levels of test compounds were assayed by a LC/MS method. In this method, an aliquot of plasma was treated by mixing with acetonitrile to precipitate protein, centrifuged to clarify the supernatant and then further diluted with formate buffer (50 mM) and injected onto an HPLC. Test compounds were separated from endogenous interfering substances and subsequently eluted from the HPLC column for mass spectrometric quantification.

Microsomal Incubations. Nicotine adenine dinucleotide phosphate (NADPH)-dependent transformation was studied with concentrations of 100 μM of test compound. Incubations were conducted at 37 °C and contained 2 mg/mL of liver microsomal protein in pH 7.4, 40 mM phosphate buffer containing 3 mM

magnesium chloride and 1.0 mM NADPH. Aliquots of the incubations were taken at specific time points over a 30 min incubation period. To stop the reaction the timed aliquots were added to an equal volume of acetonitrile containing an internal standard (IS). The IS-acetonitrile solution denatured and precipitated the microsomal protein. The protein was separated by centrifugation, and an aliquot of the resultant supernatants were assayed by a HPLC/UV method. Incubations prepared without the addition of NADPH acted as controls.

Acknowledgment. The Advanced Light Source is supported by the Director, Office of Science, Office of Basic Energy Sciences, Materials Sciences Division, of the U.S. Department of Energy under Contract No. DE-AC03-76SF00098 at Lawrence Berkeley National Laboratory.

Supporting Information Available: Results from elemental analysis. This material is available free of charge via the Internet at <http://pubs.acs.org>

References

- (1) (a) Adams, J. L.; Badger, A. M.; Kumar, S.; Lee, J. C. p38 MAP kinase: molecular target for the inhibition of pro-inflammatory cytokines. *Prog. Med. Chem.* **2001**, *38*, 1–60. (b) Schett, G.; Tohidast-Akrad, M.; Smolen, J. S.; Schmid, B. J.; Steiner, C.; Bitzan, P.; Zenz, P.; Redlich, K.; Xu, Q.; Steiner, G. Activation, differential localization, and regulation of the stress-activated protein kinases, extracellular signal-regulated kinase, c-Jun N-terminal kinase, and p38 mitogen-activated protein kinase, in synovial tissue and cells in rheumatoid arthritis. *Arthritis Rheumatism*. **2000**, *43*, 2501–2512. (c) Foster, M. L.; Halley, F.; Souness, J. E. Potential of p38 inhibitors in the treatment of rheumatoid arthritis. *Drug News Perspect.* **2000**, *13*, 488–497. (d) Chakravarty, S.; Dugar, S. Inhibitors of p38 α MAP kinase. *Annu. Rep. Med. Chem.* **2002**, *37*, 177–186. (e) Dinarello, C. A. Inflammatory cytokines: Interleukin-1 and tumor necrosis factor as effector molecules in autoimmune diseases. *Curr. Opin. Immunol.* **1991**, *3*, 941–948.
- (2) (a) Feldmann, M. B.; Fionula M.; Maini, Ravinder N. Role of cytokines in rheumatoid arthritis. *Annu. Rev. Immunol.* **1996**, *14* 397–440. (b) Maini, R. N. The role of tumour necrosis factor in rheumatoid arthritis. *Cytokines and Joint Injury* **2004**, 1–28. (c) Toussiot, E.; Wendling, D. The use of TNF- α blocking agents in rheumatoid arthritis: an overview. *Expert Opin. Pharmacother.* **2004**, *5*(3), 581–594. (d) Rutgeerts, P.; van Assche, G.; Vermeire, S. Optimizing anti-TNF treatment in inflammatory bowel disease. *Gastroenterology* **2004**, *126*(6), 1593–1610. (e) Leonard, C. L.; Powers, J. L.; Matheson, R. T.; Goffe, B. S.; Zitnik, R.; Wang, A.; Gottlieb, A. B. Etanercept as monotherapy in patients with psoriasis. *New Eng. J. Med.* **2003**, *349*(21), 2014–2022 (f) Weinberg, J. M. An overview of infliximab, etanercept, efalizumab, and alefacept as biologic therapy for psoriasis. *Clin. Therapeut.* **2003**, *25*(10), 2487–2505 (g) Pincus, T.; Ferraccioli, G.; Sokka, T.; Larsen, A.; Rau, R.; Kushner, I.; Wolfe, F. Evidence from clinical trials and long-term observational studies that disease-modifying anti-rheumatic drugs slow radiographic progression in rheumatoid arthritis: updating a 1983 review. *Rheumatology* **2002**, *41*(12), 1346–1356. (h) Hallegua, D. S.; Weisman, M. H. Potential therapeutic uses of interleukin 1 receptor antagonists in human diseases. *Ann. Rheum. Dis.* **2002**, *61*(11), 960–967.
- (3) (a) Saklatvala, J. The p38 MAP kinase pathway as a therapeutic target in inflammatory disease. *Curr. Op. in Pharm.* **2004**, *4*(4), 372–377. (b) Kumar, S.; Blake, S. M. Pharmacological potential of p38 MAPK inhibitors. *Handbook Exp. Pharm.* **2005**, *167*, 65–83.
- (4) Weisman M, F. D.; Schiff M.; Kauffman R.; Merica E.; Martin-Munley S. FRI0018 A double-blind, placebo-controlled trial of VX-745, an oral p38 mitogen activated protein kinase (MAPK) inhibitor, in patients with rheumatoid arthritis (RA) *Ann. Rheum. Diseases* **2002**, *61*, Suppl. 1
- (5) (a) Amakye, D. T., S.; Ward, C. Pharmacokinetics (PK) and pharmacodynamics (PD) of SCIO-469, a p38 gamma MAP kinase inhibitor. *Clin. Pharmacol. Therapeut.* **2004**, *75*, 3. (b) Gupta, A.; Yong, C.; Madwed, J. B.; Staehle, H.; Wood, C. C. Safety, pharmacokinetics and pharmacodynamics of single doses of an oral p38 MAP kinase inhibitor (BIRB 796 BS) in healthy human males a placebo-controlled, randomized study, double blinded at each dose level. *J. Allergy Clin. Immunol.* **2002**, *109* (1) 365–375 (c) Parasrampur, D. A.; de Boer, P.; Desai-Krieger, D.; Chow, A. T.; Jones, C. R. Single-dose pharmacokinetics and pharmacodynamics of RWJ 67657, a specific p38 mitogen-activated protein kinase inhibitor: a first-in-human study. *J. Clin. Pharmacol.* **2003**, *43* (4), 406–413

- (6) Trejo, A.; Arzeno, H.; Browner, M.; Chanda, S.; Cheng, S.; Comer, D. D.; Dalrymple, S. A.; Dunten, P.; Lafargue, J.; Lovejoy, B.; Freire-Moar, J.; Lim, J.; McIntosh, J.; Miller, J.; Papp, E.; Reuter, D.; Roberts, R.; Sanpablo, F.; Saunders, J.; Song, K.; Villasenor, A.; Warren, S. D.; Welch, M.; Weller, P.; Whiteley, P. E.; Zeng, L.; Goldstein, D. M. Design and Synthesis of 4-Azaindoles as Inhibitors of p38 MAP Kinase. *J. Med. Chem.* **2003**, 46(22), 4702–4713.
- (7) Conrow, R.; Portoghese, P. S. Efficient preparation of polyfunctional α -diketones from carboxylic acids. *J. Org. Chem.* **1986**, 51(6), 938–40.
- (8) Collins, P. R.; Janowski, W. K.; Prager, R. H. The chemistry of phthalide-3-carboxylic acid. VI. The stereochemistry of some 3-(aminoaryl)methylphthalides and the derived 3-aryl-4-hydroxy-3,4-dihydroisoquinolin-1(2H)-ones. *Aust. J. Chem.* **1989**, 42(4), 549–59.
- (9) Vaultier, M.; Knouzi, N.; Carrie, R. Reduction of azides to primary amines by a general method using the Staudinger reaction. *Tetrahedron Lett.* **1983**, 24(8), 763–4.
- (10) Thorand, S.; Krause, N. Improved procedures for the palladium-catalyzed coupling of terminal alkynes with aryl bromides (Sonogashira coupling). *J. Org. Chem.* **1998**, 63, 3(23), 8551–8553. (b) Sonogashira, K.; Tohda, Y.; Hagihara, N. Convenient synthesis of acetylenes. Catalytic substitutions of acetylenic hydrogen with bromo alkenes, iodo arenes, and bromopyridines. *Tetrahedron Lett.* **1975**, 50, 4467–70.
- (11) McKean, D. R.; Parrinello, G.; Renaldo, A. F.; Stille, J. K.. Synthesis of functionalized styrenes via palladium-catalyzed coupling of aryl bromides with vinyl tin reagents. *J. Org. Chem.* **1987**, 52, 2(3), 422–4.
- (12) Van Rheenen, V.; Kelly, R. C.; Cha, D. Y. An improved catalytic osmium tetroxide oxidation of olefins to *cis*-1, 2-glycols using tertiary amine oxides as the oxidant. *Tetrahedron Lett.* **1976**, 23, 1973–76.
- (13) Giroux, A.; Han, Y.; Prasit, P. One pot biaryl synthesis via in situ boronate formation. *Tetrahedron Lett.* **1997**, 38(22), 3841–3844.
- (14) Fabian, M. A.; Biggs, W. H.; Treiber, D. K.; Atteridge, C. E.; Azimioara, M. D.; Benedetti, M. G.; Carter, T. A.; Ciceri, P.; Edeen, P. T.; Floyd, M.; Ford, J. M.; Galvin, M.; Gerlach, Jay L.; Grotzfeld, R. M.; Herrgard, S.; Insko, D. E.; Insko, M. A.; Lai, A. G.; Lelias, J.; Mehta, S. A.; Milanov, Z. V.; Velasco, A. M.; Wodicka, L. M.; Patel, H. K.; Zarrinkar, P. P.; Lockhart, D. J. A small molecule-kinase interaction map for clinical kinase inhibitors. *Nature Biotechnol.* **2005**, 23, 329–336.
- (15) Otwinowski, Z.; Minor, W. Processing of X-ray Diffraction Data Collected in Oscillation Mode. In *Methods in Enzymology*; Carter, C. W., Sweet, R. M., Eds.; Macromolecular Crystallography, part A, Academic Press: New York, 1997; Vol. 276, pp 307–326.
- (16) Brunger, A. T.; Adams, P. D.; Clore, G. M.; Delano, W. L.; Gros, P.; Grosse-Kunstleve, R. W.; Jiang, J.-S.; Kuszewski, J.; Nilges, M.; Pannu, N. S.; Read, R. J.; Rice, L. M.; Simonson, T.; Warren, G. L. Crystallography & NMR system: A new software system for macromolecular structure determination. *Acta Crystallogr.* **1998**, D54, 905–921.
- (17) Berman, H. M.; Westbrook, J.; Feng, Z.; Gilliland, G.; Bhat, T. N.; Weissig, H.; Shindyalov, I. N.; Bourne, P. E. The Protein Data Bank. *Nucleic Acid Res.* **2000**, 28, 235–242.
- (18) DeLano, W. L. The PyMOL Molecular Graphics System. DeLano Scientific, San Carlos, CA, 2002; <http://www.pymol.org>.
- (19) Reimund, J. M., et al. *Gut* **1996**, 39, 684–689.
- (20) Gallagher, T. F.; Seibel, G. L.; Kassiss, S.; Laydon, J. T.; Blumenthal, M.; Lee, J. C.; Lee, D.; Boehm, J. C.; Fier-Thompson, S. M.; et al. Regulation of stress-induced cytokine production by pyridinylimidazoles; inhibition of CSBP kinase. *Bioorg. Med. Chem.* **1997**, 5 (1), 49–64.

JM050736C